

Rotation angles of a rotating disc

– A toy model exhibiting the geometric phase –

Takuya Matsumoto^{*}, Hiroki Takada[†], Osami Yasukura[‡]

^{*,‡} *Department of Applied Physics, Faculty of Engineering, University of Fukui, 3-9-1 Bunkyo, Fukui-shi, Fukui 910-8507, Japan*

^{*} *Department of Fundamental Engineering for Knowledge-Based Society, Graduate School of Engineering, University of Fukui, 3-9-1 Bunkyo, Fukui-shi, Fukui 910-8507, Japan*

[†] *Department of Human and Artificial Intelligent Systems (HART), Graduate School of Engineering, University of Fukui, 3-9-1 Bunkyo, Fukui-shi, Fukui 910-8507, Japan*

E-mail: {^{*}takuyama, [†]takada, [‡]yasukura}@u-fukui.ac.jp

Abstract

In this paper, we consider a simple kinematic model, which is a rotating disc on the edge of another fixed disc without slipping, and study the rotation angle of the rotating disc. The rotation angle consists of two parts, the dynamical phase Δ_d and the geometric phase Δ_g . The former is a dynamical rotation of the disc itself, and the geometric motion of the disc characterizes the latter. In fact, Δ_g is regarded as the geometric phase appearing in several important contexts in physics. The clue to finding the explicit form of Δ_g is the Baumkuchen lemma, which we called. Due to the Gauss-Bonnet theorem, in the case that the rotating disc comes back to the initial position, Δ_g is interpreted as the signed area of a two-sphere enclosed by the trajectory of the Gauss vector, which is a unit normal vector on the moving disc. We also comment on typical models sharing the common underlying structure, which include Foucault's pendulum, Dirac's monopole potentials, and Berry phase. Hence, our model is a very simple but distinguished one in the sense that it embodies the essential concepts in differential geometry and theoretical physics such as the Gauss-Bonnet theorem, the geometric phase, and the fiber bundles.

Contents

1	Introduction	2
2	Set up the model	3
2.1	Definition of the model	3
2.2	Dynamical phase and geometric phase	5
2.2.1	Observations	5
2.2.2	Dynamical phase and geometric phase	6
3	Solving the model	7
3.1	Baumkuchen lemma	8
3.2	Gauss map and the regularized curve	12
3.3	Connection matrix and the geodesic curvature	15
3.4	Main theorem	17
4	Applications for some examples	21
4.1	Collection of the results	21
4.2	Examples	22
5	Some models sharing the common structure	28
5.1	Foucault's pendulum and its generalization	29
5.2	Dirac's monopole potential	31
5.3	Berry phases	35
6	Concluding remarks	36
A	Alternative proof of Theorem 3.15	38
B	Baumkuchen angle and the geodesic curvature	39

1 Introduction

It is not easy to be aware of something that exists around us like the air. The *geometric phase* is a phase shift which an object acquires when it moves in spacetime, and it only depends on the geometric property of the orbit. Though the existence is ubiquitous in physics, it seemed to take a long time for us to recognize its significance. Interestingly, the notion has been pointed out in pretty different contexts in physics, such as classical optics [1], molecular physics [2], classical physics [3], and quantum mechanics [4, 5]. For a comprehensive review, see [6]. This reflects that the geometric phase is a universal phenomena in physics.

From a mathematical point of view, the geometric phase is regarded as the *holonomy* of the fiber bundles. Concerning the mathematical background of differential geometry and topology, see [7, 8, 9, 10]. Hence, the difficulty in noticing the geometric phase is that of *seeing* the fiber in the real world. The simplest but nontrivial example of the principal fiber bundle is the *Hopf fibration* [11], which is S^1 fibration over S^2 and whose total space is S^3 .

In 1931, the same year when the Hopf fibration was proposed, Dirac has considered the *magnetic monopole potential*, which is the vector potential describing the magnetic monopole, and shown that all electric charges should be quantized if the magnetic monopole exists [12]. Dirac's quantization condition is explained as the topological consistency condition of the *gauge transformation* of the $U(1)$ principal fiber [13, 14]. For a review of Dirac's monopole, see, for instance, [15]. Furthermore, the monopole potential is entirely interpreted as the connection one-form of the Hopf fibration [16, 17].

In this paper, we consider a simple kinematic model, which is a rotating disc on the edge of another fixed disc without slipping, and study how the moving disc has rotated during its motion (see Fig. 1). We shall decompose the total rotation angle into two parts, the *dynamical phase* Δ_d and the *geometric phase* Δ_g . The former is a dynamical rotation of the disc itself, and the geometric motion of the disc characterizes the latter. This factor Δ_g is indeed regarded as the geometric phase that appears in several essential contexts in physics, as mentioned above. The clue to finding the explicit form of Δ_g (Def.-Thm. 3.2) is Lem. 3.1, which we call *Baumkuchen lemma*.

To reveal the geometric meaning of Δ_g , we shall introduce the Gauss map (Def. 3.4), which defines a unit normal vector on the moving disc. Consequently, it is given by the line integral of the geodesic curvature along the curve drawn by the Gauss vector on a two-sphere (Thm. 3.11). Furthermore, due to the *Gauss-Bonnet theorem*, in the case that the rotating disc comes back to the original position, Δ_g turns out to be the area of a two-sphere enclosed by the trajectory of the Gauss vector. That is the claim of our main theorem Thm. 3.15 in §3.

We will also comment on typical models sharing the common underlying mathematical structure, which include Foucault’s pendulum, Dirac’s monopole potentials, and Berry phase in §4. In particular, our approach naturally explains the *Foucault’s sine law* and leads us to propose its generalization. In this sense, our model is a straightforward but outstanding one because it embodies the essential concepts in differential geometry and theoretical physics such as the Gauss-Bonnet theorem, the geometric phase, and the fiber bundles.

This article is organized as follows. In §2, we set up the model, which is a rotating disc around a fixed disc, and explain the question that we would like to answer. Then we propose our fundamental problem. We solve the model in §3, and give the complete answer to the fundamental question, which is Thm.3.15 in §3.4. We examine how our solution works for some concrete motions of the rotating disc in §4. In §5, we explain that some essential physical models share the common mathematical structure, which contain Foucault’s pendulum, Dirac’s monopole potentials, and Berry phase. In this sense, our model is *not* an isolated one. The relation between the Hopf fibration and our model is mentioned in §6. App. A is devoted to an alternative proof of Thm.3.15. In App. B, we elucidate how our Baumkuchen lemma is related to the geodesic curvature.

2 Set up the model

Let us start to formulate our kinematical model. We define the model in §2.1. In §2.2, we introduce the notion of the dynamical phase and the geometric phase after some observations.

2.1 Definition of the model

We consider the following model,¹ which we refer to as “*Rotation angles of a rotating disc.*”

¹This model was initially proposed as one of the common problems for the 32nd Japan Mathematics Contest and the 25th Japan Junior Mathematics Contest [18].

Rotation angles of a rotating disc

Consider a disc A with the radius $a > 0$ on $z = 0$ plane (*i.e.* xy -plane) in three-dimensional space \mathbb{R}^3 and the center is located at the origin. Set another disc B in \mathbb{R}^3 with the radius $b > 0$ so that it contacts disc A at $(a \cos \theta, a \sin \theta, 0) \in \mathbb{R}^3$ with $\theta \in \mathbb{R}$. Suppose that the perpendicular line through the center of disc B must be parallel to or cross at some point with the z -axis. Denote the angle between $z = 0$ plane and the disc B by β , and suppose that $0 \leq \beta \leq \pi$, see Fig.1. The position of disc B is entirely determined by two parameters θ and β .

Let disc B rotate on the edge of disc A without slipping.

Introduce the time parameter $t \in [0, 1] \subset \mathbb{R}$ to describe this motion, and regard the angle variables θ, β as the continuous functions of t . Then, the position of the rigid body, disc B, is determined by the map

$$(\theta, \beta) : [0, 1] \rightarrow \mathbb{R} \times [0, \pi], \quad t \mapsto (\theta(t), \beta(t)). \quad (\text{M})$$

Set $\theta(0) = 0$. Starting at $t = 0$, disc B returns to the initial position at $t = 1$. That is

$$\theta(1) = 2\pi n \quad \text{with} \quad n \in \mathbb{Z}, \quad \beta(1) = \beta(0). \quad (\text{T})$$

We shall call the integer $\theta(1)/2\pi = n$ the *topological number*.

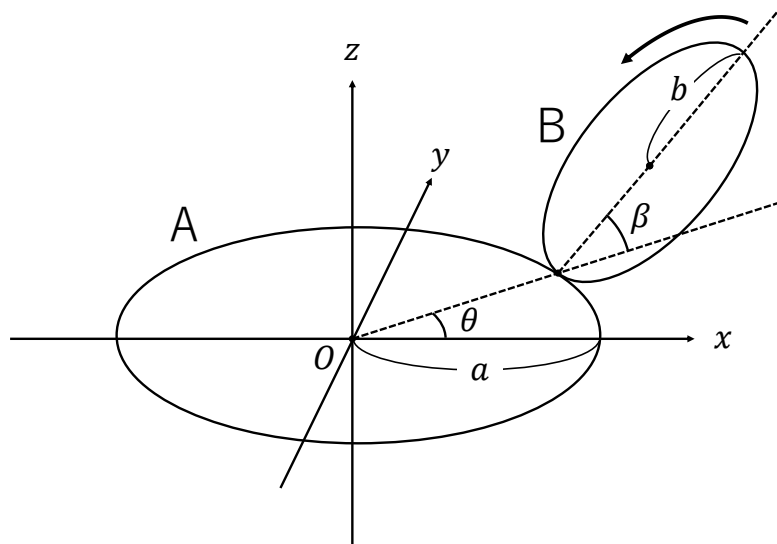


Figure 1: Disc A is fixed on xy -plane and disc B rolls on the edge of the disc A without slipping.

Remark 2.1. For the functions $\theta(t), \beta(t)$, it is supposed to meet the following conditions.

1. The continuous functions $\theta(t), \beta(t)$ satisfy the *Lipschitz condition*. That is, for any $t_1, t_2 \in [0, 1]$, there exists a positive constant C_f such that

$$|f(t_1) - f(t_2)| \leq C_f |t_1 - t_2|, \quad (2.1)$$

where f is either θ or β .

2. Both $\theta(t)$ and $\beta(t)$ are differentiable except finite number of points on $(0, 1)$. The derivatives $\theta'(t), \beta'(t)$ are piecewise continuous on $[0, 1]$.

These two conditions are physically natural. Since $t \in [0, 1]$ is an auxiliary parameter to describe the motion (M), it is always possible to assume that $\theta(t), \beta(t)$ satisfy the above conditions.

Our interest is the next question.

Question

How much does the disc B rotate in this motion from $t = 0$ to $t = 1$? Define and determine the rotation angle Δ .

2.2 Dynamical phase and geometric phase

Before considering the generic cases, let us begin to examine some elementary cases. We will observe that the rotation angle Δ consists of two parts, *i.e.*, the *dynamical* phases and the *geometric* phases.

2.2.1 Observations

The typical cases are that the angle β is constant in the motion (M). Here, we shall have a look at three cases, (i) $\beta = 0$, (ii) $\beta = \pi/2$, and (iii) $\beta = \pi$.

- (i) In the first case $(\theta, \beta) = (2\pi t, 0)$, two discs A and B are on the same plane, $z = 0$. The contacting point of two discs moves counterclockwise, starting from $(a, 0, 0)$ and turning back to the same point. The length of the contacting point traveling is $2\pi a$. Hence, dividing it by the radius of the disc B, we get the rotation angle $2\pi b/a$. However, in addition to this angle, disc B turns around disc A by 2π , which equals the rotation angle of disk B if discs A and B are glued at the contacting point and they rotate together. Thus, the total rotation angle is given by

$$\Delta = \frac{2\pi a}{b} + 2\pi. \quad (2.2)$$

In particular, if two radii of discs are equal $a = b$, then it reduces to

$$\Delta = 2\pi + 2\pi = 4\pi, \quad (2.3)$$

which means that disc B is rotating *twice!* The readers can confirm this fact experimentally by using two coins on a desk. Put one coin on a desk and fix it with one hand. Then, turn another around the fixed one so that it does not slip on the edge. You will see that the moving coin rotates twice when it comes back to the original position.

- (ii) The second case $(\theta, \beta) = (2\pi t, \pi/2)$ corresponds that disc B is vertical to disc A. In this case, the rotation angle of disk B is 0 if it is slipping at the contacting point. Hence, since disk B is not slipping at the contacting point, it totally rotates by

$$\Delta = \frac{2\pi a}{b}. \quad (2.4)$$

If $a = b$, it simply becomes

$$\Delta = 2\pi. \quad (2.5)$$

This means that disc B only rotates just *once*. It is also possible to see this fact with two coins on a table, but it would require more concentration and careful treatment.

- (iii) For the third case $(\theta, \beta) = (2\pi t, \pi)$, though the contacting point walks the same length, $2\pi a$, as the case (i), disc B rotates inside of disc A. This direction of the rotation is opposite to the first case. Thus, the total rotation angle is given by

$$\Delta = \frac{2\pi a}{b} - 2\pi. \quad (2.6)$$

When $a = b$, the rotation angle vanishes

$$\Delta = 2\pi - 2\pi = 0. \quad (2.7)$$

This can be explained by the two-coin experiment as follows. In this case, one coin is just upon another. Since they are the same size, we cannot move the coin above without it slipping.

2.2.2 Dynamical phase and geometric phase

The previous three examples imply that the total rotation angle Δ of disc B consists of two components. One component is the factor $2\pi a/b$. This is the ratio of the length of the curve which the contacting point of two discs moves to the radius of disc B. We call this *the dynamical phase* and denote it by Δ_d . The dynamical phase commonly appears in any case. In general, it is given by

Definition-Proposition 2.2. *The dynamical phase for the motion (M) with the topological condition (T) is given by*

$$\Delta_d = \frac{2\pi na}{b}. \quad (2.8)$$

Proof. For the motion (M) satisfying the topological condition (T), the signed length of the curve which the contacting point of two discs moves is

$$a \int_0^1 \frac{d\theta(t)}{dt} dt = a(\theta(1) - \theta(0)) = 2\pi na. \quad (2.9)$$

Dividing this by the radius b , we obtain Δ_d . □

Since $\theta(t) = 2\pi t$ and the topological number is $n = 1$ for the above examples (i), (ii), and (iii), the dynamical phase reads $\Delta_d = 2\pi a/b$.

While, another component is independent of the ratio a/b , and it only depends on how disc B has moved in \mathbb{R}^3 . In other words, this component reflects the geometric aspect of the motion (M). Hence, we refer to this as *the geometric phase* and express it by Δ_g . In summary, the total rotation angle Δ of disc B is decomposed as

$$\begin{aligned} \Delta &= \Delta_d + \Delta_g, \quad \text{with} \\ \Delta_d &= \frac{2\pi na}{b} \text{ (dynamical phase)}, \quad \Delta_g = \text{(geometric phase)}. \end{aligned} \quad (2.10)$$

Therefore, our question essentially reduces to the following problem.

Fundamental Problem

Determine the geometric phase Δ_g for arbitrary motion (M) with the topological condition (T).

3 Solving the model

Since we have defined the model in the previous section, we shall solve the model. In §3.1, we propose our key lemma 3.1, *Baumkuchen lemma* and give the explicit formula for the geometric phase in Def.-Thm. 3.2. Next, to elucidate the geometric meaning, we introduce the notion of the Gauss map (Def.3.4) and the regularized curve (Def.3.5) in §3.2. In §3.3, we prepare some crucial tools, the connections matrix and the geodesic curvature. With these preparations, in §3.4, the main theorem 3.15 will be proved.

3.1 Baumkuchen lemma

We shall adopt the following trivial fact as a cornerstone of our subsequent arguments, what we call *Baumkuchen lemma*.

Lemma 3.1 (Baumkuchen lemma). *Consider two fans OAA' and OBB' with the same center O , and suppose that A, B, O and A', B', O are on the same lines. (See Fig 2.) Let q be the length $AB = A'B'$, which is the width of a piece of Baumkuchen, and denote the lengths of the arcs $\widehat{AA'}$ and $\widehat{BB'}$ by L and L_q , respectively. Then, the center angle $\theta_B = \angle AOA' = \angle BOB'$ is given by*

$$\frac{L - L_q}{q} = \theta_B. \quad (3.1)$$

In particular, the Baumkuchen angle θ_B is independent of the width q .

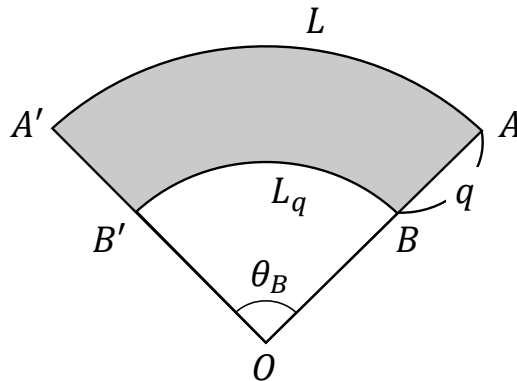


Figure 2: The angle θ_B of two edges AB and $A'B'$ of a piece of *Baumkuchen* is obtained by dividing the difference of the arc lengths $L - L_q$ by the width q .

Proof. Denote the radius of the fan by $OA = OA' = r$. Since $L = r\theta_B$ and $L_q = (r - q)\theta_B$, we get

$$\frac{L - L_q}{q} = \frac{r\theta_B - (r - q)\theta_B}{q} = \theta_B. \quad (3.2)$$

This is, of course, independent of q . □

Answer for the Fundamental Problem is obtained by using Lem. 3.1. The purpose here is to prove the following theorem.

Definition-Theorem 3.2. *The geometric phase of the motion (M) is given by*

$$\Delta_g = \int_0^1 \cos \beta(t) \frac{d\theta(t)}{dt} dt. \quad (3.3)$$

Proof. First, we decompose the time interval $[0, 1]$ into a mesh consisting of N segments such that

$$0 = t_0 < t_1 < \cdots < t_k < \cdots < t_{N-1} < t_N = 1. \quad (3.4)$$

The typical choice of a mesh would be given by

$$t_k = \frac{k}{N} \quad \text{with} \quad k = 0, 1, \dots, N. \quad (3.5)$$

Second, we apply Baumkuchen lemma 3.1 for each segment $[t_k, t_{k+1}]$ with $0 \leq k \leq N - 1$. On the segment $[t_k, t_{k+1}]$, we may assume that $\beta(t)$ is constant for a sufficiently large N . Let B be the center of disc B, P the contacting point of discs A and B at $t = t_k$, and they respectively move to B' and P' at $t = t_{k+1}$. Now, we must notice that there is a Baumkuchen with two arcs $\widehat{BB'}$ and $\widehat{PP'}$. The infinitesimal motion of disc B is illustrated in Fig. 3. The infinitesimal geometric phase of disc B is identified with the Baumkuchen angle θ_B . Since $AP = a$, $PB = b$ in Fig. 3a, the arc lengths $\widehat{BB'}$, $\widehat{PP'}$ read respectively as

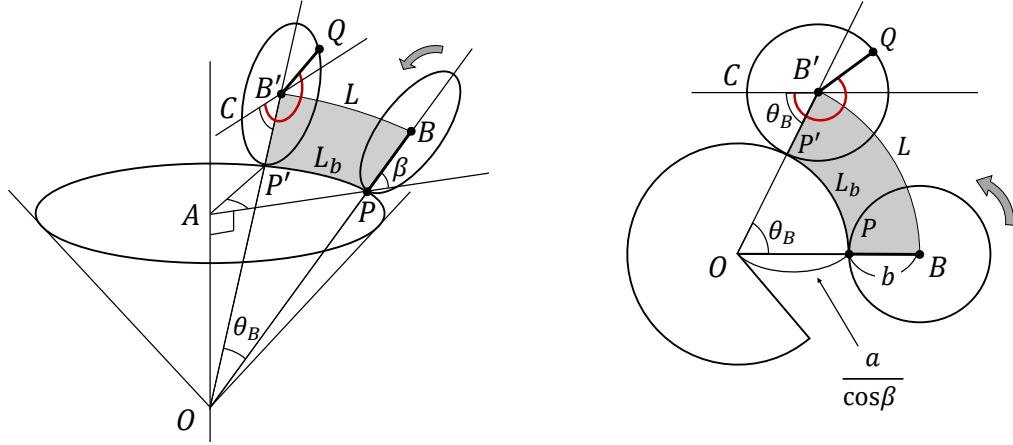
$$\begin{aligned} L &= \widehat{BB'} = (a + b \cos \beta(t_k))(\theta(t_{k+1}) - \theta(t_k)), \\ L_b &= \widehat{PP'} = a(\theta(t_{k+1}) - \theta(t_k)). \end{aligned} \quad (3.6)$$

Here, we have regarded the radius of disc B as the width of Baumkuchen, namely $q = b$. Thus, by the Baumkuchen lemma 3.1, the geometric phase can be calculated as

$$\theta_B = \frac{L - L_b}{b} = \cos \beta(t_k)(\theta(t_{k+1}) - \theta(t_k)). \quad (3.7)$$

Third, we obtain the total geometric phase Δ_g by summing up these infinitesimal angles for all k . To be precise, define $\beta_k^{\text{out}}, \beta_k^{\text{in}}$ for $0 \leq k \leq N - 1$ by

$$\begin{aligned} \cos \beta_k^{\text{out}} &= \begin{cases} \max\{ \cos \beta(t) \mid t_k \leq t \leq t_{k+1} \} & \text{if } \theta(t_k) \leq \theta(t_{k+1}) \\ \min\{ \cos \beta(t) \mid t_k \leq t \leq t_{k+1} \} & \text{if } \theta(t_k) > \theta(t_{k+1}) \end{cases}, \\ \cos \beta_k^{\text{in}} &= \begin{cases} \min\{ \cos \beta(t) \mid t_k \leq t \leq t_{k+1} \} & \text{if } \theta(t_k) \leq \theta(t_{k+1}) \\ \max\{ \cos \beta(t) \mid t_k \leq t \leq t_{k+1} \} & \text{if } \theta(t_k) > \theta(t_{k+1}) \end{cases}. \end{aligned} \quad (3.8)$$



(a) Baumkuchen appears as a part of the cone. The angle $\angle PAP'$ is $\theta(t_{k+1}) - \theta(t_k)$.

(b) Baumkuchen is in the fan, an open cone in the flat space. Here, CB' is parallel to OB and hence $\theta_B = \angle POP' = \angle CB'P'$.

Figure 3: The infinitesimal motion of disc B in $[t_k, t_{k+1}]$. Cutting the cone in Fig. 3a along the line OP , we obtain Fig. 3b. The Baumkuchen is indicated by grey. The total rotation angle $\angle CB'Q$ in red is given by the sum of the Baumkuchen angle θ_B and the dynamical angle $\angle P'B'Q$. The point P at t_k on disc B travels to the point Q at t_{k+1} .

Let $\Delta_g^{(k)}$ be the infinitesimal geometric phase for the time segment $[t_k, t_{k+1}]$. By definition, the following holds,

$$\cos \beta_k^{\text{in}} (\theta(t_{k+1}) - \theta(t_k)) \leq \Delta_g^{(k)} \leq \cos \beta_k^{\text{out}} (\theta(t_{k+1}) - \theta(t_k)). \quad (3.9)$$

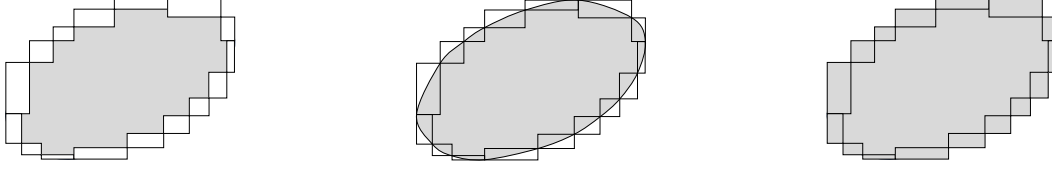
Summing up for k , we get

$$\Delta_{g,N}^{\text{in}} \leq \Delta_g \leq \Delta_{g,N}^{\text{out}}, \quad (3.10)$$

where we have denoted

$$\begin{aligned} \Delta_{g,N}^{\text{in}} &= \sum_{k=0}^{N-1} \cos \beta_k^{\text{in}} (\theta(t_{k+1}) - \theta(t_k)), & \Delta_g &= \sum_{k=0}^{N-1} \Delta_g^{(k)}, \\ \Delta_{g,N}^{\text{out}} &= \sum_{k=0}^{N-1} \cos \beta_k^{\text{out}} (\theta(t_{k+1}) - \theta(t_k)). \end{aligned} \quad (3.11)$$

Both $\Delta_{g,N}^{\text{in}}$ and $\Delta_{g,N}^{\text{out}}$ are the bounded monotone sequences with respect to N , and they converge to the same value. See Fig. 4. In fact, it is evaluated as



(a) Area measured by $\Delta_{g,N}^{\text{in}}$. (b) Area measured by Δ_g . (c) Area measured by $\Delta_{g,N}^{\text{out}}$.

Figure 4: The areas measured by $\Delta_{g,N}^{\text{in}}$, Δ_g , $\Delta_{g,N}^{\text{out}}$ are indicated in grey in Figures (a), (b), (c), respectively. The horizontal direction is θ and the vertical is $\cos \beta$. The sign of Δ_g is positive if the boundary is oriented clockwise.

$$\begin{aligned}
|\Delta_{g,N}^{\text{out}} - \Delta_{g,N}^{\text{in}}| &\leq \sum_{k=0}^{N-1} |\cos \beta_k^{\text{out}} - \cos \beta_k^{\text{in}}| |\theta(t_{k+1}) - \theta(t_k)| \\
&\leq \sum_{k=0}^{N-1} |\beta_k^{\text{out}} - \beta_k^{\text{in}}| |\theta(t_{k+1}) - \theta(t_k)|.
\end{aligned} \tag{3.12}$$

Since $\beta(t)$ is continuous, for any $\epsilon > 0$, there exists an enough large N such that

$$|\beta_k^{\text{out}} - \beta_k^{\text{in}}| < \epsilon. \tag{3.13}$$

In addition, due to the Lipschitz conditions for $\theta(t)$ in Rem. 2.1, there exists a positive constant C_θ such that

$$|\theta(t_{k+1}) - \theta(t_k)| \leq C_\theta(t_{k+1} - t_k) = \frac{C_\theta}{N}. \tag{3.14}$$

Then, we have

$$|\Delta_{g,N}^{\text{out}} - \Delta_{g,N}^{\text{in}}| \leq \frac{\epsilon C_\theta}{N}, \tag{3.15}$$

which implies that

$$|\Delta_{g,N}^{\text{out}} - \Delta_{g,N}^{\text{in}}| \rightarrow 0 \quad (N \rightarrow \infty). \tag{3.16}$$

Hence, by the squeezing lemma, we get

$$\Delta_g = \lim_{N \rightarrow \infty} \Delta_{g,N}^+ = \lim_{N \rightarrow \infty} \Delta_{g,N}^-. \tag{3.17}$$

This proves the geometric phase Δ_g is equal to the line integral in (3.3). \square

Though the above theorem gives us an explicit formula for the geometric phase, the geometric meaning is opaque. We shall elaborate on this point in the following subsections.

Remark 3.3. Fig. 3 intuitively explains the reason why the total rotation angle Δ of disc B is given by the sum of the dynamical phase Δ_d and the geometric phase Δ_g as claimed in (2.10). Opening up the cone along the line OP in Fig. 3a, we get a fan in Fig. 3b. In Fig. 3b, the total rotation angle can be decomposed into

$$\Delta = \angle CB'Q = \angle CB'P' + \angle P'B'Q. \quad (3.18)$$

Since the two line BO and CB' are parallel, the angle $\angle CB'P'$ is identified with the geometric phase,

$$\Delta_g = \angle CB'P' = \angle POP' = \theta_B. \quad (3.19)$$

On the other hand, the angle $\angle P'B'Q$ corresponds to the dynamical phase because of

$$\Delta_d = \angle P'B'Q = \frac{\widehat{P'Q}}{b} = \frac{\widehat{P'P}}{b}. \quad (3.20)$$

3.2 Gauss map and the regularized curve

Gauss map

First, we introduce the unit normal vector of disc B by *the Gauss map*, which detects the motion of disc B. We assume that two-sphere S^2 is embedded in \mathbb{R}^3 as

$$S^2 = \{ x^2 + y^2 + z^2 = 1 \mid \begin{pmatrix} x \\ y \\ z \end{pmatrix} \in \mathbb{R}^3 \} \subset \mathbb{R}^3.$$

Definition 3.4 (Gauss map). For the two parameters (θ, β) in the motion (M), define *the Gauss map* from $\mathbb{R} \times [0, \pi]$ to two-sphere S^2 by²

$$\mathbb{R} \times [0, \pi] \rightarrow S^2 \subset \mathbb{R}^3, \quad (\theta, \beta) \mapsto \mathbf{g}(\theta, \beta) = \begin{pmatrix} \sin \beta \cos \theta \\ \sin \beta \sin \theta \\ -\cos \beta \end{pmatrix}. \quad (3.21)$$

The vector $\mathbf{g}(\theta, \beta)$ is called *the Gauss vector*.

The Gauss vector is geometrically realized both in the rotating model and two-sphere as in Fig. 5a and Fig. 5b, respectively.

²The range of the angle variable β is restricted in $[0, \pi]$ in our paper. If we relax this condition from $[0, \pi]$ to $[0, 2\pi]$, we may need to consider a torus T^2 rather than a sphere S^2 as the target space of the Gauss map. The geometric phases on a torus are investigated in [19].

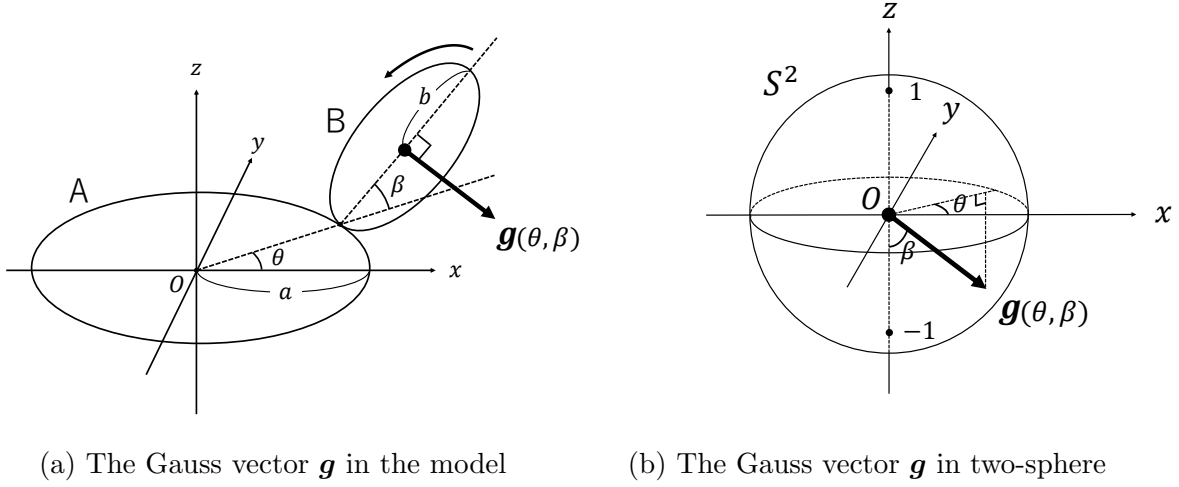


Figure 5: The Gauss map \mathbf{g} from the model (a) to two-sphere (b)

Note that $\mathbf{g}(\theta, \beta)$ is a unit vector and perpendicular to disc B. By composing the motion (M) and the Gauss map (3.21), the Gauss vector could be regarded as a function of $t \in [0, 1]$,

$$\mathbf{g} : [0, 1] \rightarrow S^2, \quad t \mapsto \mathbf{g}(t) = \begin{pmatrix} \sin \beta(t) \cos \theta(t) \\ \sin \beta(t) \sin \theta(t) \\ -\cos \beta(t) \end{pmatrix}. \quad (3.22)$$

We also refer to the map (3.22) as the Gauss map.

Because of $\mathbf{g}(1) = \mathbf{g}(0)$, the Gauss map defines the oriented closed curve γ on S^2 associated with the given motion (M) by

$$\gamma = \{ \mathbf{g}(t) \in S^2 \mid t \in [0, 1] \} \subset S^2. \quad (3.23)$$

The orientation of γ is induced from that of the parameter $t \in [0, 1]$ such as from $t = 0$ to $t = 1$. The curve γ is said to be *simple* if it does not intersect with itself.

The regularized curve

Second, let us introduce the *cut-off* with a sufficiently small ϵ ($0 < \epsilon < \pi/8$) by

$$\beta_\epsilon : [0, 1] \rightarrow [\epsilon, \pi - \epsilon], \quad t \mapsto \beta_\epsilon(t),$$

$$\beta_\epsilon(t) = \begin{cases} \epsilon & (0 \leq \beta(t) \leq \epsilon) \\ \beta(t) & (\epsilon < \beta(t) < \pi - \epsilon) \\ \pi - \epsilon & (\pi - \epsilon \leq \beta(t) \leq \pi). \end{cases} \quad (3.24)$$

The regularized Gauss vector is then given by replacing $\beta(t)$ by $\beta_\epsilon(t)$ as

$$\mathbf{g}_\epsilon : [0, 1] \rightarrow S^2 - \{0, 0, \pm 1\}, \quad t \mapsto \mathbf{g}_\epsilon(t) = \begin{pmatrix} \sin \beta_\epsilon(t) \cos \theta(t) \\ \sin \beta_\epsilon(t) \sin \theta(t) \\ -\cos \beta_\epsilon(t) \end{pmatrix}. \quad (3.25)$$

Definition 3.5 (Regularized curve). The *regularized curve* is defined by the orbit of the regularized Gauss vector,

$$\gamma(\epsilon) = \{ \mathbf{g}_\epsilon(t) \in S^2 - \{(0, 0, \pm 1)\} \mid t \in [0, 1] \} \subset S^2 - \{(0, 0, \pm 1)\}. \quad (3.26)$$

The point is that the curve $\gamma(\epsilon)$ dodges the poles $(0, 0, \pm 1)$, though the undeformed curve γ does not in general. By taking $\epsilon \rightarrow 0$, it reduces to the original path,

$$\gamma(\epsilon) \rightarrow \gamma. \quad (3.27)$$

Proposition 3.6. *The geometric phase for the motion (M) is given by the limit of the line integral along the regularized curve $\gamma(\epsilon)$ in (3.26),*

$$\Delta_g = \lim_{\epsilon \rightarrow 0} \int_{\gamma(\epsilon)} \cos \beta_\epsilon d\theta \quad (3.28)$$

Proof. The right hand side is calculated as

$$\lim_{\epsilon \rightarrow 0} \int_{\gamma(\epsilon)} \cos \beta_\epsilon d\theta = \lim_{\epsilon \rightarrow 0} \int_0^1 \cos \beta_\epsilon(t) \frac{d\theta(t)}{dt} dt = \int_0^1 \cos \beta(t) \frac{d\theta(t)}{dt} dt. \quad (3.29)$$

By Def.-Thm. 3.2, this coincides with the geometric phase Δ_g . \square

Remark 3.7. The regularized curve $\gamma(\epsilon)$ always and uniquely exists for the motion (M). Note that, in some cases, two mutually different curves $\gamma_1(\epsilon), \gamma_2(\epsilon)$ give rise to the same curve γ in $\epsilon \rightarrow 0$ limit *i.e.*,

$$\lim_{\epsilon \rightarrow 0} \gamma_1(\epsilon) = \lim_{\epsilon \rightarrow 0} \gamma_2(\epsilon) = \gamma. \quad (3.30)$$

However, the resulting geometric phases do *not* coincide in general,

$$\lim_{\epsilon \rightarrow 0} \int_{\gamma_1(\epsilon)} \cos \beta d\theta \neq \lim_{\epsilon \rightarrow 0} \int_{\gamma_2(\epsilon)} \cos \beta d\theta. \quad (3.31)$$

This is because the Gauss vector \mathbf{g} cannot detect the motion when it is at the poles $(0, 0, \pm 1)$. In this sense, the regularized Gauss vector \mathbf{g}_ϵ in (3.25) more faithfully describes the motion of disc B. In other words, the geometric phase Δ_g is a functional of curve γ , but it is *not* continuous for the infinitesimal variation of γ . Indeed, the discontinuity by $\pm 2\pi n$ ($n \in \mathbb{Z}$) occurs when the curve γ jumps over the poles at $(0, 0, \pm 1)$. Examples (v) and (iv) in § 4.2 will demonstrate what we have mentioned here.

3.3 Connection matrix and the geodesic curvature

Next, we shall elucidate the geometric meaning of the one-form $\cos \beta d\theta$ in (3.28).

Connection matrix

Using the Gauss vector (3.21), we introduce the local orthonormal frame of \mathbb{R}^3 at $\mathbf{g}(\theta, \beta) \in S^2$ by

$$\begin{aligned} \mathbf{e}_1 &= \frac{\partial \mathbf{g}}{\partial \theta} / \left| \frac{\partial \mathbf{g}}{\partial \theta} \right| = \begin{pmatrix} -\sin \theta \\ \cos \theta \\ 0 \end{pmatrix}, & \mathbf{e}_2 &= \frac{\partial \mathbf{g}}{\partial \beta} / \left| \frac{\partial \mathbf{g}}{\partial \beta} \right| = \begin{pmatrix} \cos \beta \cos \theta \\ \cos \beta \sin \theta \\ \sin \beta \end{pmatrix}, \\ \mathbf{e}_3 &= \mathbf{e}_1 \times \mathbf{e}_2 = \begin{pmatrix} \sin \beta \cos \theta \\ \sin \beta \sin \theta \\ -\cos \beta \end{pmatrix}. \end{aligned} \quad (3.32)$$

It is noticed that $\mathbf{e}_3 = \mathbf{g}$ and they satisfy

$$\begin{aligned} \mathbf{e}_i \cdot \mathbf{e}_j &= \delta_{ij} \quad (i, j = 1, 2, 3), \\ \mathbf{e}_1 \times \mathbf{e}_2 &= -\mathbf{e}_2 \times \mathbf{e}_1 = \mathbf{e}_3, \quad \mathbf{e}_2 \times \mathbf{e}_3 = -\mathbf{e}_3 \times \mathbf{e}_2 = \mathbf{e}_1, \quad \mathbf{e}_3 \times \mathbf{e}_1 = -\mathbf{e}_1 \times \mathbf{e}_3 = \mathbf{e}_2. \end{aligned} \quad (3.33)$$

Noting that the vectors \mathbf{e}_1 and \mathbf{e}_2 are always oriented to the *east* and *north*, respectively, and \mathbf{e}_3 is to the *sky*. In particular, \mathbf{e}_1 and \mathbf{e}_2 span the tangent space $T_{\mathbf{g}}S^2$.

The *connection matrix* (ω_{ij}) is defined by

$$\begin{pmatrix} d\mathbf{e}_1 \\ d\mathbf{e}_2 \\ d\mathbf{e}_3 \end{pmatrix} = \begin{pmatrix} \omega_{11} & \omega_{12} & \omega_{13} \\ \omega_{21} & \omega_{22} & \omega_{23} \\ \omega_{31} & \omega_{32} & \omega_{33} \end{pmatrix} \begin{pmatrix} \mathbf{e}_1 \\ \mathbf{e}_2 \\ \mathbf{e}_3 \end{pmatrix}. \quad (3.34)$$

By the orthonormal condition (3.33), it immediately follows that ω is anti-symmetric

$$\omega_{ij} = -\omega_{ji} = d\mathbf{e}_i \cdot \mathbf{e}_j \quad \text{for } i, j = 1, 2, 3. \quad (3.35)$$

It is explicitly calculated as

$$\begin{pmatrix} \omega_{11} & \omega_{12} & \omega_{13} \\ \omega_{21} & \omega_{22} & \omega_{23} \\ \omega_{31} & \omega_{32} & \omega_{33} \end{pmatrix} = \begin{pmatrix} 0 & -\cos \beta d\theta & -\sin \beta d\theta \\ \cos \beta d\theta & 0 & -d\beta \\ \sin \beta d\theta & d\beta & 0 \end{pmatrix}. \quad (3.36)$$

In particular, we see that $\omega_{21} = \cos \beta d\theta$. Hence, by Prop. 3.6, we have the following proposition.

Proposition 3.8. *It holds that*

$$\Delta_g = \lim_{\epsilon \rightarrow 0} \int_{\gamma(\epsilon)} \omega_{21}. \quad (3.37)$$

Reparameterization from t to s

To describe the motion of disc B, it is convenient to adopt the *length* of the curve γ rather than the *time* parameter $t \in [0, 1]$. We shall express the length parameter by $s \in [0, L(\gamma)]$, where $L(\gamma)$ is the length of $\gamma \subset S^2$, and regard $\mathbf{g}(s)$ as a function of the length s rather than the time t . The orientation of the curve parametrized by s is induced from that of the time parameter t such that

$$\mathbf{g}(t)|_{t=0} = \mathbf{g}(s)|_{s=0} \quad \text{and} \quad \mathbf{g}(t)|_{t=1} = \mathbf{g}(s)|_{s=L(\gamma)}. \quad (3.38)$$

On an open neighborhood for a fixed $t \in (0, 1)$, where $\mathbf{g}(t)$ is differentiable and $\mathbf{g}'(t) \neq 0$, the length parameter s is related to the time parameter t via the reparameterization

$$s : [0, 1] \rightarrow [0, L(\gamma)], \quad t \mapsto s(t) \quad \text{such that} \quad |\mathbf{g}'(s)| = |\mathbf{g}'(t)| \frac{dt}{ds} = 1. \quad (3.39)$$

By the definition, the speed of $\mathbf{g}(s)$ is normalized as 1 for the parameter s . We also see that ds^2 is the line element of S^2 . By (3.39) and (3.36), we have

$$ds = |\mathbf{g}'(t)| dt, \quad \mathbf{g}'(t) = \frac{d\mathbf{e}_3}{dt} = \sin \beta \frac{d\theta}{dt} \mathbf{e}_1 + \frac{d\beta}{dt} \mathbf{e}_2. \quad (3.40)$$

Therefore, we obtain

$$ds^2 = \sin^2 \beta d\theta^2 + d\beta^2. \quad (3.41)$$

This is nothing but the line element of S^2 in terms of the local coordinate (θ, β) . In the subsequent argument, we reserve s for the length parameter.

Geodesic curvature

Due to $|\mathbf{g}'(s)| = 1$ and $\mathbf{g}'(s) \in T_{\mathbf{g}(s)}S^2 = \text{span}\{\mathbf{e}_1, \mathbf{e}_2\}$, let us express the tangent vector $\mathbf{g}'(s)$ by using an angle φ ,

$$\mathbf{g}'(s) = \cos \varphi \mathbf{e}_1 + \sin \varphi \mathbf{e}_2, \quad \text{where} \quad \cos \varphi = \sin \beta \frac{d\theta}{ds}, \quad \sin \varphi = \frac{d\beta}{ds}. \quad (3.42)$$

See Fig. 6. Replacing φ by $\varphi + \pi/2$, we have the orthogonal vector defined by

$$\boldsymbol{\nu}(s) = -\sin \varphi \mathbf{e}_1 + \cos \varphi \mathbf{e}_2. \quad (3.43)$$

Note that they satisfy

$$|\mathbf{g}'(s)| = |\boldsymbol{\nu}(s)| = 1, \quad \mathbf{g}'(s) \cdot \boldsymbol{\nu}(s) = 0. \quad (3.44)$$

The relation between the local frames $\{\mathbf{e}_1, \mathbf{e}_2\}$ and $\{\mathbf{g}'(s), \boldsymbol{\nu}(s)\}$ is presented in Fig. 6. Differentiating the second relation, we get

$$\mathbf{g}''(s) \cdot \boldsymbol{\nu}(s) + \mathbf{g}'(s) \cdot \boldsymbol{\nu}'(s) = 0. \quad (3.45)$$

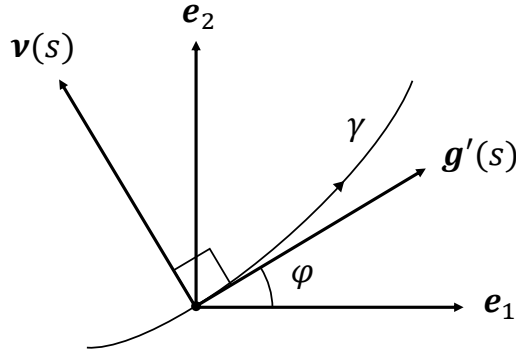


Figure 6: The moving frames $\{\mathbf{g}'(s), \boldsymbol{\nu}(s)\}$ and $\{\mathbf{e}_1, \mathbf{e}_2\}$ at $\mathbf{g}(s) \in S^2$. The vectors \mathbf{e}_1 and \mathbf{e}_2 are oriented to the east and north, respectively. φ is the angle between the local frames.

Definition 3.9 (Geodesic curvature). The *geodesic curvature* of $\gamma \subset S^2$ at $\mathbf{g}(s) \in \gamma$ is defined by

$$\kappa_g(s) = \mathbf{g}''(s) \cdot \boldsymbol{\nu}(s) = -\mathbf{g}'(s) \cdot \boldsymbol{\nu}'(s). \quad (3.46)$$

Now, let us calculate the geodesic curvature explicitly. Plugging (3.42) and

$$\boldsymbol{\nu}'(s)ds = -\cos \varphi(d\varphi + \omega_{12}) \mathbf{e}_1 - \sin \varphi(d\varphi + \omega_{12}) \mathbf{e}_2 + (-\sin \varphi \omega_{13} + \cos \varphi \omega_{23}) \mathbf{e}_3, \quad (3.47)$$

with the geodesic curvature (3.46), we obtain

$$\kappa_g(s)ds = d\varphi + \omega_{12}. \quad (3.48)$$

The above argument can be summarized in the following proposition.

Proposition 3.10. *The infinitesimal geometric phase $\cos \beta d\theta$ in (3.28), the element ω_{21} of the connection matrix (3.36), the angle φ in (3.42), and the geometric curvature $\kappa_g(s)ds$ in (3.46) satisfy the relation*

$$\cos \beta d\theta = \omega_{21} = d\varphi - \kappa_g(s)ds. \quad (3.49)$$

3.4 Main theorem

By Prop.3.6, the geometric phase is obtained by evaluating the line integral along the regularized curve $\gamma(\epsilon)$ and taking the regularization parameter ϵ to zero. It is, however, noticed that the curve $\gamma(\epsilon)$ is piecewise smooth in general and could have finite cusp points. Let us suppose that the curve $\gamma(\epsilon)$ has $n(\epsilon) \in \mathbb{Z}_{\geq 0}$ cusp points and, at the i -th cusp point,

denote the external angle to the counterclockwise by $\alpha_i(\epsilon)$. Define the geodesic curvature $\kappa_g^\epsilon(s)$ for $\gamma(\epsilon) \subset S^2 - \{(0, 0, \pm 1)\}$ at $\mathbf{g}_\epsilon(s) \in \gamma(\epsilon)$ by

$$\kappa_g^\epsilon(s) = \mathbf{g}_\epsilon''(s) \cdot \boldsymbol{\nu}_\epsilon(s) = -\mathbf{g}_\epsilon'(s) \cdot \boldsymbol{\nu}_\epsilon'(s), \quad (3.50)$$

where $\boldsymbol{\nu}_\epsilon(s)$ is the normalized orthogonal vector to $\mathbf{g}_\epsilon'(s)$ as similar in (3.43).

Then, the geometric phase is given by

$$\Delta_g = \lim_{\epsilon \rightarrow 0} \int_{\gamma(\epsilon)} d\varphi - \lim_{\epsilon \rightarrow 0} \left(\int_{\gamma(\epsilon)} \kappa_g^\epsilon ds + \sum_{i=1}^{n(\epsilon)} \alpha_i(\epsilon) \right). \quad (3.51)$$

Since the second term reduces to the line integral on the undeformed curve γ , we can express the geometric phase as follows.

Theorem 3.11. *The geometric phase for the motion (M) is evaluated by*

$$\Delta_g = \lim_{\epsilon \rightarrow 0} \int_{\gamma(\epsilon)} d\varphi - \int_{\gamma} \kappa_g ds - \sum_{i=1}^n \alpha_i. \quad (3.52)$$

Here, γ in (3.23) is the trajectory of the Gauss vector, $\gamma(\epsilon)$ introduced in (3.26) is the regularized curve of γ avoiding the poles $(0, 0, \pm 1)$, φ defined in (3.42) is the angle of the tangent vector of γ measured from the local orthogonal frame, κ_g defined in (3.46) is the geodesic curvature of γ , and α_i is the external angle to counterclockwise at the i -th cusp point of γ .

Remark 3.12. Theorem 3.11 is valid not only for a closed curve γ , but also for some open paths *not* satisfying the topological condition (T). However, when γ is closed, an interesting geometric interpretation exists. That is the claim of Theorem 3.15.

When the closed curve $\gamma(\epsilon)$ does not intersect with itself, *i.e.*, simple, it defines two region $S_+(\epsilon)$ and $S_-(\epsilon)$ on S^2 such as

$$S^2 = S_+(\epsilon) \cup S_-(\epsilon), \quad \gamma(\epsilon) = S_+(\epsilon) \cap S_-(\epsilon), \quad \partial S_+(\epsilon) = -\partial S_-(\epsilon) = \gamma(\epsilon). \quad (3.53)$$

Note that $S_+(\epsilon)$ is the region surrounded by the oriented curve $\gamma(\epsilon)$ on the left hand side. Let us call $(0, 0, 1)$ and $(0, 0, -1)$ the *north* and *south pole*, respectively. Since the regularized curve $\gamma(\epsilon)$ does not pass through the north and south poles, it makes sense to introduce the indices $I_\pm \in \{0, 1, 2\}$ as the number of poles included in $S_\pm(\epsilon)$. By definition, it holds

$$I_+ + I_- = 2. \quad (3.54)$$

Using the indices I_{\pm} , we can express the first term on the right hand side of (3.52) as

$$\int_{\gamma(\epsilon)} d\varphi = -\pi(I_+ - I_-) = \begin{cases} 2\pi & ((I_+, I_-) = (0, 2)) \\ 0 & ((I_+, I_-) = (1, 1)) \\ -2\pi & ((I_+, I_-) = (2, 0)) \end{cases}. \quad (3.55)$$

Since the results are stable under the deformation of parameter ϵ , we have

Lemma 3.13.

$$\lim_{\epsilon \rightarrow 0} \int_{\gamma(\epsilon)} d\varphi = -2\pi I_+ + 2\pi = 2\pi I_- - 2\pi = -\pi(I_+ - I_-). \quad (3.56)$$

Next, let us consider the second and third terms on the right hand side in (3.52). Denote the areas of $S_{\pm}(\epsilon)$ by $A_{\pm}(\epsilon)$, respectively, and set $S_{\pm}(0) = S_{\pm}$, $A_{\pm}(0) = A_{\pm}$. Since the area of two-sphere is 4π , it holds that

$$A_+(\epsilon) + A_-(\epsilon) = 4\pi. \quad (3.57)$$

With these notations, applying the *Gauss-Bonnet theorem* for $S_+(\epsilon)$, we obtain

$$\int_{S_+(\epsilon)} K dA + \int_{\partial S_+(\epsilon)} \kappa_g ds + \sum_{i=1}^{n(\epsilon)} \alpha_i(\epsilon) = 2\pi \chi(S_+(\epsilon)), \quad (3.58)$$

where K is the *Gauss curvature*, $dA = \sin \beta d\theta \wedge d\beta$ is the volume form of S^2 , and $\chi(S_+(\epsilon))$ is the *Euler characteristic* of $S_+(\epsilon)$ which is topologically isomorphic to a closed unit disc. Since $K = 1$ for two-sphere, the first term on the left hand side is equal to the area of $S_+(\epsilon)$,

$$\int_{S_+(\epsilon)} K dA = \int_{S_+(\epsilon)} \sin \beta d\theta \wedge d\beta = A_+(\epsilon). \quad (3.59)$$

Taking into account $\chi(S_+(\epsilon)) = 1$, we have

$$-\int_{\partial S_+(\epsilon)} \kappa_g ds - \sum_{i=1}^{n(\epsilon)} \alpha_i(\epsilon) = A_+(\epsilon) - 2\pi. \quad (3.60)$$

By sending $\epsilon \rightarrow 0$, we obtain

Lemma 3.14.

$$-\int_{\gamma} \kappa_g ds - \sum_{i=1}^n \alpha_i = A_+ - 2\pi = -A_- + 2\pi = \frac{A_+ - A_-}{2}. \quad (3.61)$$

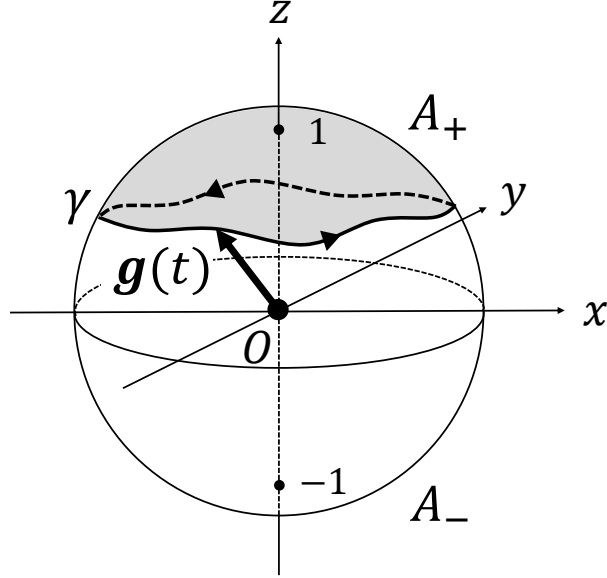


Figure 7: The curve γ in S^2 appears as a trajectory of the Gauss vector $\mathbf{g}(t)$ whose orientation is induced by the parameter t . A_+ is the area enclosed by γ on the left side, while A_- is on the right. The topological index $I_+(I_-)$ is the number of poles $(0, 0, \pm 1)$ contained in γ on the left (right, respectively). In the above picture, $I_+ = I_- = 1$.

We are now ready to state our main theorem, which solves the Fundamental Problem.

Theorem 3.15 (Main Theorem). *Suppose that the oriented closed curve γ defined in (3.23) is simple. Then, for the motion (M), the geometric phase is given by*

$$\Delta_g = A_+ - 2\pi I_+ = -A_- + 2\pi I_- = \frac{A_+ - A_-}{2} - \pi(I_+ - I_-). \quad (3.62)$$

Proof. Applying Lem. 3.13 and Lem. 3.14 for Thm. 3.11, we immediately get

$$\Delta_g = (-2\pi I_+ + 2\pi) + (A_+ - 2\pi) = A_+ - 2\pi I_+. \quad (3.63)$$

The other expressions easily follow from $A_+ + A_- = 4\pi$ and $I_+ + I_- = 2$. \square

Our answer to the question is given below.

Answer for the Question

The rotation angle Δ of the rotating disc B in the motion (M) with the topological condition (T) is given by the sum of the dynamical phase Δ_d and the geometric phase Δ_g as follows,

$$\Delta = \Delta_d + \Delta_g \quad \text{with} \quad \Delta_d = \frac{2\pi na}{b}, \quad \Delta_g = A_+ - 2\pi I_+. \quad (3.64)$$

Here, A_+ is the area of the region surrounded by the curve γ in (3.23) which is supposed to be simple, and $I_+ \in \{0, 1, 2\}$ is a number of the poles enclosed by the regularized curve $\gamma(\epsilon)$ in (3.26) on the left side.

Remark 3.16. If γ is not simple, Δ_g is obtained by decomposing it into the sum of simple closed curves and repeatedly applying the formula (3.64) for each segment.

4 Applications for some examples

In this section, we apply our solution for the typical motions. After collecting the results we have obtained so far in §4.1, we will apply them to six examples in §4.2.

4.1 Collection of the results

The total rotation angle Δ consists of the dynamical phase Δ_d and the geometric phase Δ_g , that is $\Delta = \Delta_d + \Delta_g$ in (2.10). The dynamical phase is given by

$$\Delta_d = \frac{a\theta(1)}{b} = \frac{2\pi na}{b}, \quad (\text{Def.-Prop. 2.2})$$

and the geometric phase is

$$\Delta_g = A_+ - 2\pi I_+, \quad (\text{Thm. 3.15 (Main theorem)})$$

where A_+ is the area surrounded by the curve $\gamma \subset S^2$ on the left side, and $I_+ \in \{0, 1, 2\}$ is the number of poles enclosed by the regularized curve $\gamma(\epsilon) \subset S^2 - \{(0, 0, \pm 1)\}$. Their explicit relations are the followings,

$$A_+ = 2\pi - \int_{\gamma} \kappa_g(s) ds - \sum_{i=1}^n \alpha_i, \quad (\text{Lem. 3.14})$$

$$2\pi I_+ = 2\pi - \lim_{\epsilon \rightarrow 0} \int_{\gamma(\epsilon)} d\varphi. \quad (\text{Lem. 3.13})$$

We have gained Thm. 3.15 by rewriting

$$\Delta_g = \int_0^1 \cos \beta(t) \frac{d\theta(t)}{dt} dt = \lim_{\epsilon \rightarrow 0} \int_{\gamma(\epsilon)} \cos \beta_\epsilon d\theta \quad (\text{Def.-Thm. 3.2 and Prop. 3.6})$$

according to Prop. 3.10 and plugging the above expressions in it.

4.2 Examples

We apply the above results to some typical examples. Here, we discuss the six examples. The first four examples, (i), (ii), (iii), and (iv), treat the cases in which β is constant. While, the last two examples, (v) and (vi), focus on the cases in which β varies. All data for the rotation angles are listed in Tab. 1.

Table 1: All data to find out the rotation angles Δ for the six examples in § 4.2. Note that $\Delta = \Delta_d + \Delta_g$ and $\Delta_g = A_+ - 2\pi I_+$.

	Δ_d	A_+	$2\pi I_+$	Δ_g	Δ	Figures
(i)	$\frac{2\pi a}{b}$	4π	2π	2π	$\frac{2\pi a}{b} + 2\pi$	Fig. 8
(ii)	$\frac{2\pi a}{b}$	2π	2π	0	$\frac{2\pi a}{b}$	Fig. 9
(iii)	$\frac{2\pi a}{b}$	0	2π	-2π	$\frac{2\pi a}{b} - 2\pi$	Fig. 10
(iv)	$\frac{2\pi a}{b}$	$2\pi(1 + \cos \beta_0)$	2π	$2\pi \cos \beta_0$	$\frac{2\pi a}{b} + 2\pi \cos \beta_0$	Fig. 11
(v)	0	$\frac{\pi}{2}$	0	$\frac{\pi}{2}$	$\frac{\pi}{2}$	Fig. 12, 14, 15a
(vi)	$-\frac{2\pi a}{b}$	$\frac{\pi}{2}$	2π	$-\frac{3\pi}{2}$	$-\frac{2\pi a}{b} - \frac{3\pi}{2}$	Fig. 13, 14, 15b

The first four examples consider cases where β is constant. In the examples (i), (ii), and (iii), we shall revisit our observations in § 2.2.1. Example (iv) interpolates the three examples.

(i) The first case is the motion (M) defined by

$$\theta(t) = 2\pi t, \quad \beta(t) = 0. \quad (4.65)$$

In this case, the dynamical phase reads $\Delta_d = 2\pi a/b$. The curve γ is just a point at the *south pole* $(0, 0, -1)$, and the regularized curve $\gamma(\epsilon)$ is a small circle enclosing it on the right side. See Fig. 8. Hence, A_+ is the area of S^2 , namely 4π , and $I_+ = 1$. This yields

$$\Delta_g = A_+ - 2\pi I_+ = 4\pi - 2\pi = 2\pi. \quad (4.66)$$

Therefore, the total rotation angle is given by

$$\Delta = \Delta_d + \Delta_g = \frac{2\pi a}{b} + 2\pi. \quad (4.67)$$

(ii) The second case is defined by

$$\theta(t) = 2\pi t, \quad \beta(t) = \frac{\pi}{2}. \quad (4.68)$$

In this case, the dynamical phase reads $\Delta_d = 2\pi a/b$. The curve γ is the grand circle in $z = 0$ plane, that is the *equator* oriented from west to east. The regularized curve $\gamma(\epsilon)$ is same to γ . Hence, A_+ is the half area of S^2 , namely 2π , and $I_+ = 1$. See Fig. 9. This yields the vanishing of the geometric phase,

$$\Delta_g = A_+ - 2\pi I_+ = 2\pi - 2\pi = 0. \quad (4.69)$$

Then, the total rotation angle is given by

$$\Delta = \Delta_d + \Delta_g = \frac{2\pi a}{b} + 0 = \frac{2\pi a}{b}. \quad (4.70)$$

(iii) The third case is the motion defined by

$$\theta(t) = 2\pi t, \quad \beta(t) = \pi. \quad (4.71)$$

In this case, the dynamical phase is $\Delta_d = 2\pi a/b$, too. The curve γ is just a point at the *north pole* $(0, 0, 1)$, and the regularized curve $\gamma(\epsilon)$ is a small circle enclosing it on the left side. Hence, A_+ is zero, and $I_+ = 1$. See Fig. 10. This gives

$$\Delta_g = A_+ - 2\pi I_+ = 0 - 2\pi = -2\pi. \quad (4.72)$$

Therefore, the total rotation angle is given by

$$\Delta = \Delta_d + \Delta_g = \frac{2\pi a}{b} - 2\pi. \quad (4.73)$$

The above three examples reproduce our observations discussed in § 2.2.1. Next example interpolates these three cases.

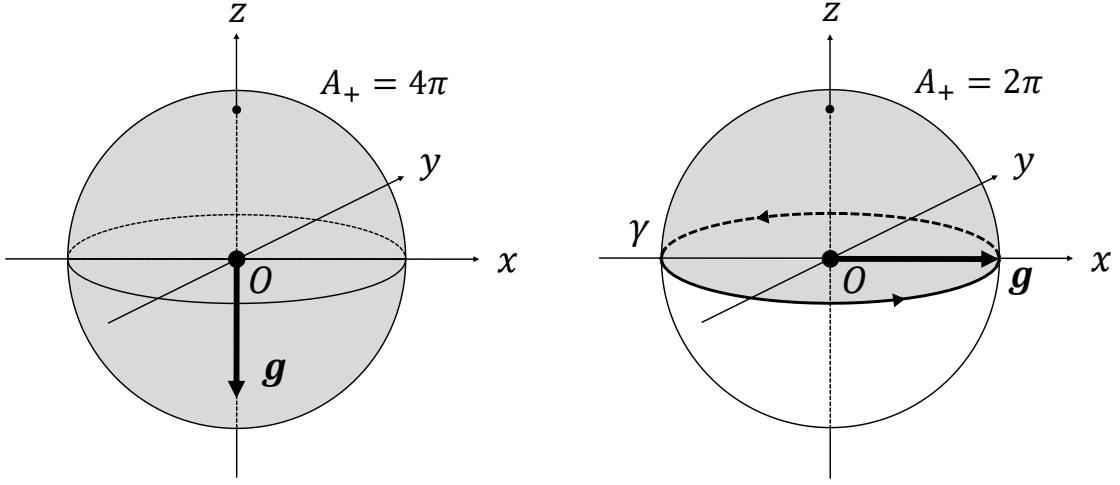


Figure 8: Area, for example (i), is 4π . Figure 9: Area, for example (ii), is 2π .
The curve γ a point at $(0, 0, -1)$. The curve γ is the equator.

(iv) The fourth case is the motion defined by

$$\theta(t) = 2\pi t, \quad \beta(t) = \beta_0, \quad (4.74)$$

where $\beta_0 \in [0, \pi]$ is constant. It is noticed that $\beta_0 = 0, \pi/2, \pi$ correspond to the cases (i), (ii), and (iii), respectively. In this case, the dynamical phase is also $\Delta_d = 2\pi a/b$. The curve γ is just a small circle with a constant *latitude*. The regularized curve $\gamma(\epsilon)$ is necessary if either $\beta_0 = 0$ or π . See Fig. 11. In this case, A_+ is the area of the spherical cap covering the north pole, which is calculated as

$$A_+ = 2\pi(1 + \cos \beta_0), \quad (4.75)$$

and $I_+ = 1$. Hence, we obtain

$$\Delta_g = A_+ - 2\pi I_+ = 2\pi(1 + \cos \beta_0) - 2\pi = 2\pi \cos \beta_0. \quad (4.76)$$

We will see how this geometric phase is relating to the *Foucault's pendulum* in § 5.1. Therefore, the total rotation angle is given by

$$\Delta = \Delta_d + \Delta_g = \frac{2\pi a}{b} + 2\pi \cos \beta_0. \quad (4.77)$$

The following two examples address cases where β changes. It is noted that they have the same closed curve γ , but the regularized curves $\gamma(\epsilon)$ are different, which give rise to the different indices I_+ . This is a concrete example of the situation mentioned in Rem. 3.7.

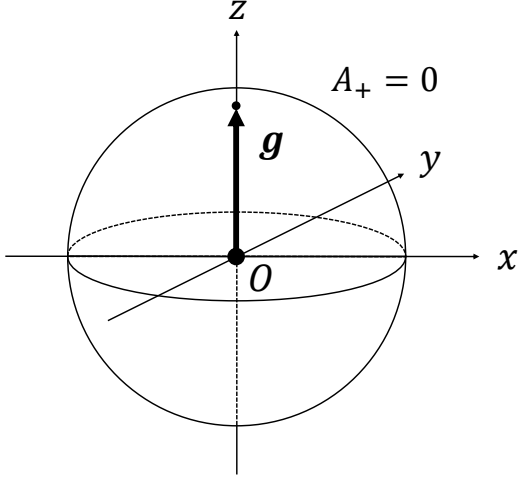


Figure 10: Area, for example (iii), is zero. The curve γ shrinks to $(0, 0, 1)$.

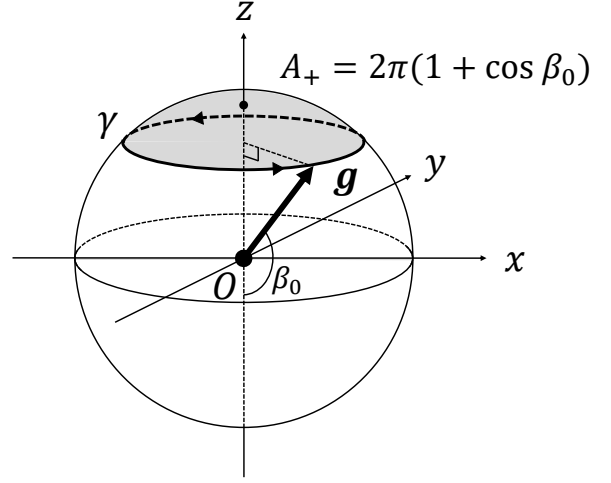


Figure 11: Area, for example (iv), is $2\pi(1 + \cos \beta_0)$. The curve γ is a circle of latitude.

(v) The fifth case is the motion defined by

$$\theta(t) = \begin{cases} 2\pi t & (0 \leq t \leq 1/4) \\ \pi/2 & (1/4 \leq t \leq 1/2) \\ 2\pi(3/4 - t) & (1/2 \leq t \leq 3/4) \\ 0 & (3/4 \leq t \leq 1) \end{cases}, \quad \beta(t) = \begin{cases} 0 & (0 \leq t \leq 1/4) \\ 2\pi(t - 1/4) & (1/4 \leq t \leq 1/2) \\ \pi/2 & (1/2 \leq t \leq 3/4) \\ 2\pi(1 - t) & (3/4 \leq t \leq 1) \end{cases}. \quad (4.78)$$

In this case, it is noticed that the dynamical phase is zero,

$$\Delta_d = \frac{a\theta(1)}{b} = 0. \quad (4.79)$$

The curve γ is a curved triangle on S^2 with one vertex at the south pole $(0, 0, -1)$ and the other two on the equator. The orientation of γ on the equator is from east to west. Every external angle at the corners is $\pi/2$, and all edges are parts of the grand circle, *i.e.*, the geodesic lines. The regularized curve $\gamma(\epsilon)$ is a curved triangle having a chip at the corner of $(0, 0, -1)$. This gives rise to $I_+ = 0$ because the south pole *is not* included in the region $S_+(\epsilon)$. See Fig. 12 and Fig. 14, where we have flipped the direction of z -axis for the explanation. On the other hand, A_+ in Fig. 14 is the $1/8$ area of S^2 , that is, $4\pi/8 = \pi/2$. Consequently, the geometric phase turns out to be

$$\Delta_g = A_+ - 2\pi I_+ = \frac{\pi}{2} - 0 = \frac{\pi}{2}. \quad (4.80)$$

Therefore, the total rotation angle is given by

$$\Delta = \Delta_d + \Delta_g = 0 + \frac{\pi}{2} = \frac{\pi}{2}. \quad (4.81)$$

In this example, it is interesting that Δ does not depend on the radii of discs a, b due to the vanishing of the dynamical phase $\Delta_d = 0$, and is equal to the geometric phase Δ_g itself.

(vi) The sixth case is the motion defined by

$$\theta(t) = \begin{cases} -6\pi t & (0 \leq t \leq 1/4) \\ -3\pi/2 & (1/4 \leq t \leq 1/2) \\ -2\pi(t + 1/4) & (1/2 \leq t \leq 3/4) \\ -2\pi & (3/4 \leq t \leq 1) \end{cases}, \quad \beta(t) = \begin{cases} 0 & (0 \leq t \leq 1/4) \\ 2\pi(t - 1/4) & (1/4 \leq t \leq 1/2) \\ \pi/2 & (1/2 \leq t \leq 3/4) \\ 2\pi(1 - t) & (3/4 \leq t \leq 1) \end{cases}. \quad (4.82)$$

In comparison with the previous example (v), $\beta(t)$ is same but $\theta(t)$ is different. In this case, the dynamical phase reads

$$\Delta_d = \frac{a\theta(1)}{b} = -\frac{2\pi a}{b}. \quad (4.83)$$

It is noted that the curve γ is exactly the same as the example (v). However, the regularized curve $\gamma(\epsilon)$ is a curved triangle with a protrusion covering the pole $(0, 0, -1)$. See Fig. 13 and Fig. 14. This yields $I_+ = 1$ because the south pole *is* contained in the region $S_+(\epsilon)$. Taking into account $A_+ = \pi/2$, we gain the geometric phase as

$$\Delta_g = A_+ - 2\pi I_+ = \frac{\pi}{2} - 2\pi = -\frac{3\pi}{2}. \quad (4.84)$$

Therefore, the total rotation angle is given by

$$\Delta = \Delta_d + \Delta_g = -\frac{2\pi a}{b} - \frac{3\pi}{2}. \quad (4.85)$$

Remark 4.1. It is worth directly evaluating the geometric phases for the above examples (v) and (iv). To calculate the integrals given in Def.-Thm. 3.2, it is sufficient to consider a mesh,

$$0 = t_0 < t_1 < t_2 < t_3 < t_4 = 1, \quad t_1 = \frac{1}{4}, \quad t_2 = \frac{1}{2}, \quad t_3 = \frac{3}{4}. \quad (4.86)$$

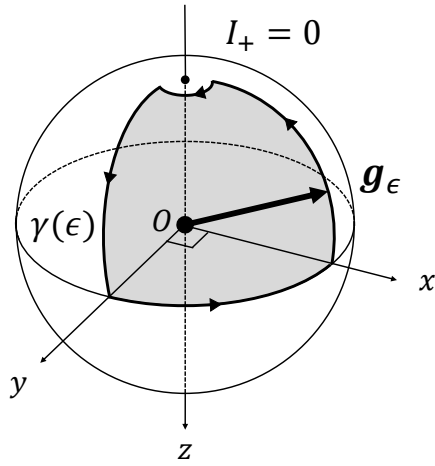


Figure 12: The regularized curve $\gamma(\epsilon)$ for example (v). The south pole *is not* contained in the grayed region $S_+(\epsilon)$, and hence $I_+ = 0$.

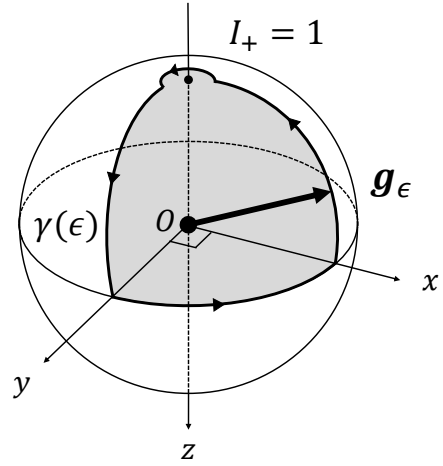


Figure 13: The regularized curve $\gamma(\epsilon)$ for example (vi). The south pole *is* contained in the grayed region $S_+(\epsilon)$, and hence $I_+ = 1$.

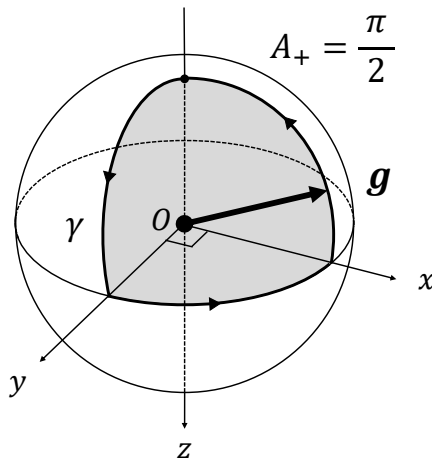
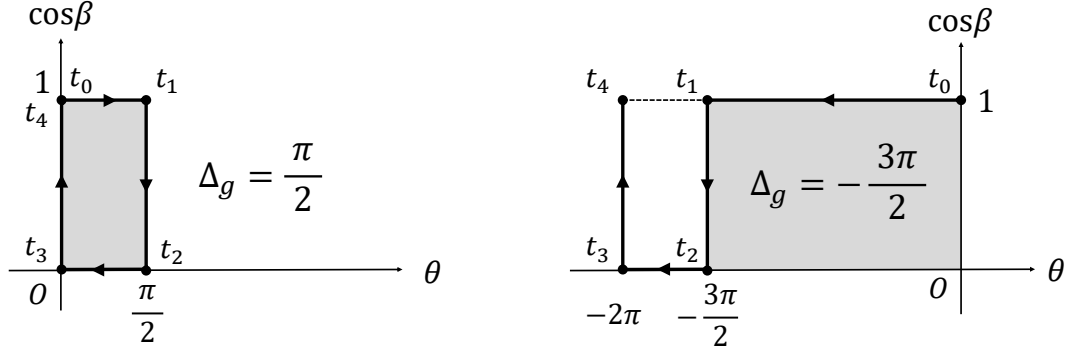


Figure 14: Areas, for both examples (v) and (vi), are $\pi/2$. The curve γ is a triangle whose edges are the geodesic lines.



(a) The line integral for example (v)

(b) The line integral for example (vi)

Figure 15: The signed areas indicated in gray give the geometric phases Δ_g . The time evolution is from $t_0 = 1$ to $t_4 = 1$ as in (4.86).

(v) For the motion defined by (4.78), it is calculated as

$$\begin{aligned}
 \Delta_g &= \int_0^1 \cos \beta(t) \frac{d\theta(t)}{dt} dt = \left[\int_0^{1/4} + \int_{1/4}^{1/2} + \int_{1/2}^{3/4} + \int_{3/4}^1 \right] \cos \beta(t) \frac{d\theta(t)}{dt} dt \\
 &= 1 \times \frac{\pi}{2} + \int_{1/4}^{1/2} \cos \beta(t) \times 0 dt + 0 \times \left(-\frac{\pi}{2}\right) + \int_{3/4}^1 \cos \beta(t) \times 0 dt \\
 &= \frac{\pi}{2}.
 \end{aligned} \tag{4.87}$$

This indeed coincides with (4.80). See Fig. 15a.

(vi) For the motion defined by (4.82), it is similarly computed as

$$\begin{aligned}
 \Delta_g &= \left[\int_0^{1/4} + \int_{1/4}^{1/2} + \int_{1/2}^{3/4} + \int_{3/4}^1 \right] \cos \beta(t) \frac{d\theta(t)}{dt} dt \\
 &= 1 \times \left(-\frac{3\pi}{2}\right) + \int_{1/4}^{1/2} \cos \beta(t) \times 0 dt + 0 \times \left(-\frac{\pi}{2}\right) + \int_{3/4}^1 \cos \beta(t) \times 0 dt \\
 &= -\frac{3\pi}{2}.
 \end{aligned} \tag{4.88}$$

This coincides with (4.84). See Fig. 15b.

5 Some models sharing the common structure

In this section, we shall elucidate that the several models exhibiting the geometric phases share the common structure with our model, which include the *Foucault's pendulum* (§ 5.1),

Dirac's monopole potentials (§5.2), and *Berry phases* (§5.3). In other words, our model extracts the underlying mathematical structures for these models.

5.1 Foucault's pendulum and its generalization

Consider a sufficiently long and heavy pendulum suspended from the high ceiling so that the oscillation would not be damped by the effect of friction. If we set the pendulum at the north pole, the plane of oscillation spontaneously rotates clockwise by 2π in 24 hours, because the earth itself rotates counterclockwise by 2π in a day. At the south pole, the pendulum rotates counterclockwise by 2π in 24 hours, while, on the equator, it remains in the same plane.

This is a famous experiment to demonstrate the earth's rotation, and often referred to as the *Foucault's pendulum* [20]. In general, the oscillation plane of the Foucault's pendulum at the latitude $\lambda \in [-\pi/2, \pi/2]$ rotates clockwise by

$$\Delta_{\text{Fou}} = 2\pi \sin \lambda, \quad (5.1)$$

in 24 hours, which is known as the *Foucault's sine law*.

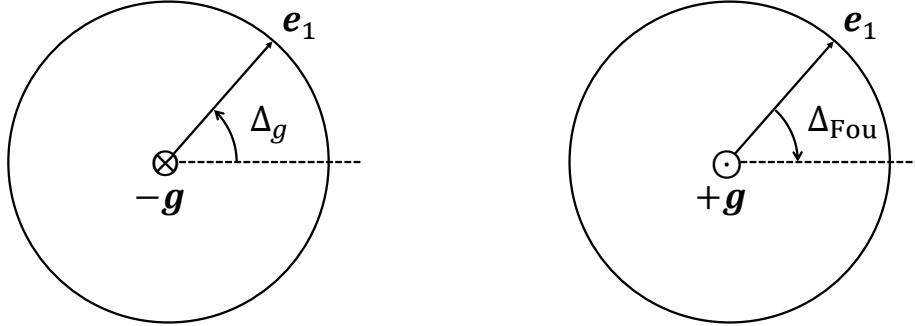
Our model can be mapped to Foucault's pendulum through the following steps.

1. By parallel transportation in \mathbb{R}^3 , we move disc B so that its center is at $\mathbf{g}(\theta, \beta) \in S^2$ and it is tangent to S^2 at the point.
2. Assume S^2 as the earth and ignore the dynamical phase Δ_d . We can regard disc B as the local frame of an observer at $\mathbf{g}(\theta, \beta) \in S^2$, namely a *compass* beneath the pendulum.
3. On the disc B, set a Foucault's pendulum. Then, the plane of the pendulum oscillation defines the local inertial frame on it.

By the above procedure, our geometric phase Δ_g can be identified with Foucault's rotation angle Δ_{Fou} . Precisely, Δ_g expresses how disc B has been forced to rotate counterclockwise observed from $-\mathbf{g}$ (Fig. 16a). On the other hand, Δ_{Fou} means how the oscillation plane, or equivalently the local inertial frame, on disc B rotates clockwise measured from $+\mathbf{g}$ (Fig. 16b). Thus, Δ_g and Δ_{Fou} measure the same angle in the opposite directions as illustrated in Fig. 16. The explicit relations of other quantities between our model and Foucault's pendulum are listed in Tab. 2.

Proposition 5.1. *Let Δ_{Fou} be the rotation angle of the Foucault's pendulum. Then, it is related to the geometric phase as*

$$\Delta_{\text{Fou}} = -\Delta_g. \quad (5.2)$$



(a) The geometric phase, Δ_g . (b) The shift of the oscillation plane, Δ_{Fou} .

Figure 16: The relation between Δ_g and Δ_{Fou} on disc B. The dotted line means the local inertial system, in which Foucault's pendulum remains.

To restore the Foucault's sine law, we map the local coordinates θ and β to the longitude $\lambda \in [0, 2\pi]$ and the latitude $\phi \in [-\pi/2, \pi/2]$, respectively, as in Tab. 2,

$$\theta = \lambda + 2\pi t, \quad \beta = \phi + \frac{\pi}{2}, \quad (5.3)$$

where time parameter t counts days. The factor $2\pi t$ means that the earth rotates by 2π in a day. Note that the motion realizing Foucault's pendulum corresponds to the example (iv) in § 4.2 and Fig. 11. Since t changes from 0 to 1 in a day, and λ, ϕ are constant, we have

$$\Delta_{\text{Fou}} = -\Delta_g = - \int_0^1 \cos\left(\phi + \frac{\pi}{2}\right) \frac{d(\lambda + 2\pi t)}{dt} dt = 2\pi \sin \phi. \quad (5.4)$$

This coincides with Foucault's sine law (5.1).

Generalized Foucault's pendulum

Prop. 5.1 implies the generalization of Foucault's pendulum. For instance, assume that a pendulum is carried on a big ship, which is still sufficient in the Pacific Ocean. The ship is sailing in the north and south directions and back to the original position 24 hours later. In this case, the sea route looks like a wavy line γ as Fig. 7. Taking into account Thm. 3.15, we gain the rotation angle of the pendulum against a compass on the ship as

$$\Delta_{\text{Fou}} = -\Delta_g = 2\pi - A_+ = A_- - 2\pi = \frac{A_- - A_+}{2}, \quad (5.5)$$

where A_+ is the area of the north side enclosed by the sea route γ , while A_- is that of the south side. This naturally explains why the oscillation plane of the pendulum on

Table 2: The correspondence between our model and the Foucault's pendulum

Our model	Foucault's pendulum
S^2	the earth
Δ_d	0
disc B	local frame of observer (a compass below the pendulum)
t	t (day)
$\theta - 2\pi t$	λ (longitude)
$\beta - \pi/2$	ϕ (latitude)
$-\Delta_g$	Δ_{Fou}

the equator does not change. When the sea route γ coincides with the equator, A_+ and A_- are the areas of the northern and southern hemispheres, respectively. Thus, due to $A_+ = A_- = 2\pi$, we get

$$\Delta_{\text{Fou}} = \frac{A_- - A_+}{2} = \frac{2\pi - 2\pi}{2} = 0. \quad (5.6)$$

It is emphasized that this is valid even if γ does *not* coincide with the equator.

We believe that our model has potential applications for the gyroscopes of airplanes or ships because Prop. 5.1 serves the theoretical prediction of the rotation angles of gyroscopes for a given route γ referred to a compass (see, for instance, [21, 22]). Explicitly, plugging the relations (5.3) with Prop. 5.1, we propose the following *generalized Foucault's sine law*.

Proposition 5.2. *Set Foucault's pendulum on a ship floating at the longitude $\lambda(t) \in [0, 2\pi]$ and the latitude $\phi(t) \in [-\pi/2, \pi/2]$, where t is a time parameter counting days. Suppose that the ship navigates quasistatically from $t = 0$ to $t = T$. During T days, the plane of the pendulum oscillation rotates clockwise referred to a compass by*

$$\Delta_{\text{Fou}} = \int_0^T \sin \phi(t) \left(\frac{d\lambda(t)}{dt} + 2\pi \right) dt. \quad (5.7)$$

Remark 5.3. H. Kamerlingh Onnes also investigated Foucault's pendulums, and the result is collected in his Ph.D. dissertation [23], see also [24]. The geometric aspects of Foucault's pendulum are argued in [25, 26], where the relation to Hopf fibration is also mentioned. The geometric approach for mechanics is addressed in [27, 28, 29, 30].

5.2 Dirac's monopole potential

The geometric phase Δ_g in our model can also be realized by the holonomy of the $U(1)$ principal bundle, which is so-called the *Dirac's monopole potential*.

We use the following local orthonormal frame given in (3.32),

$$\mathbf{e}_1 = \begin{pmatrix} -\sin \theta \\ \cos \theta \\ 0 \end{pmatrix}, \quad \mathbf{e}_2 = \begin{pmatrix} \cos \beta \cos \theta \\ \cos \beta \sin \theta \\ \sin \beta \end{pmatrix}, \quad \mathbf{e}_3 = \begin{pmatrix} \sin \beta \cos \theta \\ \sin \beta \sin \theta \\ -\cos \beta \end{pmatrix}. \quad (5.8)$$

Note that $\mathbf{e}_3 = \mathbf{g}(\theta, \beta)$. The relations between the polar coordinates (r, β, θ) and the cartesian coordinates (x, y, z) read

$$\begin{aligned} x &= r \sin \beta \cos \theta, \\ y &= r \sin \beta \sin \theta, \\ z &= -r \cos \beta. \end{aligned} \quad (5.9)$$

Definition 5.4 (Dirac's monopole potentials [12, 10]). The *Dirac's monopole potentials* are vector fields defined by

$$\mathbf{A}_\pm = \frac{\pm 1 + \cos \beta}{r \sin \beta} \mathbf{e}_1 = \frac{1}{r(r \pm z)} \begin{pmatrix} -y \\ x \\ 0 \end{pmatrix}, \quad (5.10)$$

where \mathbf{A}_+ is well-defined for $\beta \neq 0$ and $z \neq -r$, while \mathbf{A}_- is for $\beta \neq \pi$ and $z \neq r$.

Here, we have set the magnetic charge to one. By definition, \mathbf{A}_+ and \mathbf{A}_- have stringy singularities on $z \leq 0$ and $z \geq 0$ of z -axis, respectively. The following proposition tells that those potentials describe the magnetic fields generated by the magnetic monopole at the origin.

Proposition 5.5. *For the vector fields \mathbf{A}_\pm , it holds that*

$$\begin{aligned} \nabla \times \mathbf{A}_+ &= \frac{1}{r^2} \mathbf{e}_3 \quad (\beta \neq 0), \\ \nabla \times \mathbf{A}_- &= \frac{1}{r^2} \mathbf{e}_3 \quad (\beta \neq \pi). \end{aligned} \quad (5.11)$$

Next, let us consider how our model is relating to the monopole potentials. Recalling the connection matrix (3.36), we can write

$$d\theta = \frac{\omega_{31}}{\sin \beta} = \frac{1}{\sin \beta} \mathbf{e}_1 \cdot d\mathbf{g}. \quad (5.12)$$

Applying this expression for Prop. 3.6, we get

$$\Delta_g = \lim_{\epsilon \rightarrow 0} \int_{\gamma(\epsilon)} \cos \beta_\epsilon d\theta = \lim_{\epsilon \rightarrow 0} \int_{\gamma(\epsilon)} \frac{\cos \beta_\epsilon}{\sin \beta_\epsilon} \mathbf{e}_1 \cdot d\mathbf{g}_\epsilon. \quad (5.13)$$

It is noted that $\sin \beta_\epsilon \neq 0$ for $\gamma(\epsilon)$. By definition (5.10), it holds that

$$\frac{\mathbf{A}_+ + \mathbf{A}_-}{2} = \frac{\cos \beta}{r \sin \beta} \mathbf{e}_1, \quad \frac{\mathbf{A}_+ - \mathbf{A}_-}{2} = \frac{1}{r \sin \beta} \mathbf{e}_1 = \nabla \theta. \quad (5.14)$$

Here, the second relation means the the *gauge transformation* between \mathbf{A}_+ and \mathbf{A}_- on the strip covering the equator, which follows from the gradient operator in the polar coordinates

$$\nabla = \mathbf{e}_1 \frac{1}{r \sin \beta} \frac{\partial}{\partial \theta} + \mathbf{e}_2 \frac{1}{r} \frac{\partial}{\partial \beta} + \mathbf{e}_3 \frac{\partial}{\partial r}. \quad (5.15)$$

Using these relations with $r = 1$, we obtain

$$\Delta_g = \lim_{\epsilon \rightarrow 0} \int_{\gamma(\epsilon)} \frac{\mathbf{A}_+ + \mathbf{A}_-}{2} \cdot d\mathbf{g}_\epsilon = \lim_{\epsilon \rightarrow 0} \int_{\gamma(\epsilon)} (\mathbf{A}_\pm \mp \nabla \theta) \cdot d\mathbf{g}_\epsilon. \quad (5.16)$$

We see that the term stemming from the gauge transformation yields the topological number (T) because of

$$\lim_{\epsilon \rightarrow 0} \int_{\gamma(\epsilon)} \nabla \theta \cdot d\mathbf{g}_\epsilon = \lim_{\epsilon \rightarrow 0} \int_{\gamma(\epsilon)} d\theta = \theta(1) - \theta(0) = 2\pi n. \quad (5.17)$$

In summary, we arrive at the following proposition.

Proposition 5.6. *The geometric phase is obtained by the monopole potentials defined in (5.10) as*

$$\begin{aligned} \Delta_g &= \lim_{\epsilon \rightarrow 0} \int_{\gamma(\epsilon)} \frac{\mathbf{A}_+ + \mathbf{A}_-}{2} \cdot d\mathbf{g}_\epsilon \\ &= \lim_{\epsilon \rightarrow 0} \int_{\gamma(\epsilon)} \mathbf{A}_+ \cdot d\mathbf{g}_\epsilon - 2\pi n \\ &= \lim_{\epsilon \rightarrow 0} \int_{\gamma(\epsilon)} \mathbf{A}_- \cdot d\mathbf{g}_\epsilon + 2\pi n, \end{aligned} \quad (5.18)$$

where n is the topological number given in (T), \mathbf{g}_ϵ is the deformed Gauss vector in (3.25), and $\gamma(\epsilon) \in S^2 - \{(0, 0, \pm 1)\}$ is the regularized curve in (3.26).

Concluding this subsection, let us confirm the consistency of the above proposition with Thm. 3.15. Suppose that γ is a simple closed curve enclosing $(0, 0, 1)$ on the left side as Fig. 7. In this case, noting $\gamma(\epsilon) = \gamma$ and $\partial S_+ = -\partial S_- = \gamma$, we have

$$\Delta_g = \lim_{\epsilon \rightarrow 0} \int_{\gamma(\epsilon)} \frac{\mathbf{A}_+ + \mathbf{A}_-}{2} \cdot d\mathbf{g}_\epsilon = \frac{1}{2} \left[\int_{\partial S_+} \mathbf{A}_+ \cdot d\mathbf{g} - \int_{\partial S_-} \mathbf{A}_- \cdot d\mathbf{g} \right]. \quad (5.19)$$

Since these terms are equal to the areas S_{\pm} by Stokes' theorem and Prop. 5.5 with $r = 1$,

$$\int_{\partial S_{\pm}} \mathbf{A}_{\pm} \cdot d\mathbf{g} = \int_{S_{\pm}} (\nabla \times \mathbf{A}_{\pm}) \cdot \mathbf{e}_3 dS_{\pm} = A_{\pm}, \quad (5.20)$$

we obtain the expected result

$$\Delta_g = \frac{A_+ - A_-}{2}. \quad (5.21)$$

This coincides to (3.62) with $(I_+, I_-) = (1, 1)$.

As another example, consider the case $(I_+, I_-) = (0, 2)$, in which the curve γ does not contain any poles $(0, 0, \pm 1)$ on the left side. In this case, the topological number vanishes, $n = 0$. Hence, from the second relation in (5.18), we get

$$\Delta_g = \int_{\gamma=\partial S_+} \mathbf{A}_+ \cdot d\mathbf{g}_{\epsilon} - 0 = A_+ = 4\pi - A_-. \quad (5.22)$$

Again, this is consistent with (3.62).

Remark 5.7 (A simple derivation of the Dirac' monopole potential). Though the Dirac's monopole potentials (5.10) are well-known in theoretical physics and the theory of fiber bundles, it is worth addressing the heuristic derivation in our context. Let us seek a solution for the equation,

$$\nabla \times \mathbf{A} = \frac{1}{r^2} \mathbf{e}_3 \quad (5.23)$$

with the following ansatz

$$\mathbf{A} = f(\theta, \beta) \mathbf{e}_1, \quad (5.24)$$

where $f(\theta, \beta)$ is a scalar function to be determined. Applying Stokes's theorem for the spherical cap S_+ covering the north pole of a sphere with radius r , we see that

$$\int_{\partial S_+} \mathbf{A} \cdot \mathbf{e}_1 ds = \int_{S_+} (\nabla \times \mathbf{A}) \cdot \mathbf{e}_3 dS_+. \quad (5.25)$$

For $r = 1$, see Fig. 11. By the ansatz (5.24), both hand sides are simplified as follows,

$$\begin{aligned} \text{(LHS)} &= f(\theta, \beta) \int_{\partial S_+} ds = f(\theta, \beta) \times (\text{length of the edge of the cap}), \\ \text{(RHS)} &= \frac{1}{r^2} \int_{S_+} dS_+ = \frac{1}{r^2} \times (\text{area of the cap}). \end{aligned} \quad (5.26)$$

Equating these, we find the scalar factor as

$$f(\theta, \beta) = \frac{(\text{area of the cap})}{r^2 \times (\text{length of the edge of the cap})} = \frac{2\pi r^2(1 + \cos \beta)}{r^2 \times 2\pi r \sin \beta}. \quad (5.27)$$

This restores

$$\mathbf{A} = \frac{1 + \cos \beta}{r \sin \beta} \mathbf{e}_1 = \mathbf{A}_+. \quad (5.28)$$

The parallel argument for the spherical cap covering the south pole will give us \mathbf{A}_- .

5.3 Berry phases

Let us clarify the relation of our model with the *Berry phase* [1, 2, 3, 4, 5], which is a typical geometric phase in quantum mechanics.

Consider the two-level system with the Hamiltonian,

$$H = \frac{1}{r} \begin{bmatrix} z & x - iy \\ x + iy & -z \end{bmatrix} = \begin{bmatrix} -\cos \beta & e^{-i\theta} \sin \beta \\ e^{i\theta} \sin \beta & \cos \beta \end{bmatrix}, \quad (5.29)$$

where we have used the polar coordinates defined by (5.9). The eigenvalues of H are ± 1 . The eigenvectors with eigenvalue 1 are given by

$$\begin{aligned} |\psi_+\rangle &= \frac{1}{\sqrt{2r(r+z)}} \begin{bmatrix} r+z \\ x+iy \end{bmatrix} = \begin{bmatrix} \sin \frac{\beta}{2} \\ e^{i\theta} \cos \frac{\beta}{2} \end{bmatrix} & (z \neq -r, \beta \neq 0), \\ |\psi_-\rangle &= \frac{1}{\sqrt{2r(r-z)}} \begin{bmatrix} x-iy \\ r-z \end{bmatrix} = \begin{bmatrix} e^{-i\theta} \sin \frac{\beta}{2} \\ \cos \frac{\beta}{2} \end{bmatrix} & (z \neq r, \beta \neq \pi). \end{aligned} \quad (5.30)$$

These two vectors are only different by the phase factor,

$$|\psi_+\rangle = e^{i\theta} |\psi_-\rangle. \quad (5.31)$$

Since the vector $|\psi_+\rangle$ is singular at $z = -r$ or $\beta = 0$, it is well-defined on $S^2 - \{(0, 0, -1)\}$. While, the vector $|\psi_-\rangle$ is singular at $z = r$ or $\beta = \pi$, and defined on $S^2 - \{(0, 0, 1)\}$.

The *Berry connection* is then calculated as

$$\begin{aligned} \langle \psi_+ | d | \psi_+ \rangle &= \frac{i}{2} (+1 + \cos \beta) d\theta & (\beta \neq 0), \\ \langle \psi_- | d | \psi_- \rangle &= \frac{i}{2} (-1 + \cos \beta) d\theta & (\beta \neq \pi), \end{aligned} \quad (5.32)$$

where the hermitian inner product is defined by

$$\langle a | b \rangle = \bar{a}_1 b_1 + \bar{a}_2 b_2 \quad \text{for} \quad |a\rangle = \begin{bmatrix} a_1 \\ a_2 \end{bmatrix}, |b\rangle = \begin{bmatrix} b_1 \\ b_2 \end{bmatrix} \in \mathbb{C}^2. \quad (5.33)$$

These coincide with the Dirac's monopole potentials given in (5.10),

$$\langle \psi_{\pm} | d | \psi_{\pm} \rangle = \frac{i}{2} \mathbf{A}_{\pm} \cdot d\mathbf{g}. \quad (5.34)$$

Hence, for $\beta \neq 0, \pi$, it allows us to express one-form $\cos \beta d\theta$ in terms of the Berry connections,

$$\begin{aligned} \cos \beta d\theta &= -i \langle \psi_+ | d | \psi_+ \rangle - i \langle \psi_- | d | \psi_- \rangle \\ &= -2i \langle \psi_+ | d | \psi_+ \rangle - d\theta \\ &= -2i \langle \psi_- | d | \psi_- \rangle + d\theta. \end{aligned} \quad (5.35)$$

Noting the topological number stemming from the integral,

$$\lim_{\epsilon \rightarrow 0} \int_{\gamma(\epsilon)} d\theta = \theta(1) = 2\pi n, \quad (5.36)$$

we have the following proposition.

Proposition 5.8. *The geometric phase is obtained by the Berry connections given in (5.32) as*

$$\begin{aligned} \Delta_g &= -i \lim_{\epsilon \rightarrow 0} \int_{\gamma(\epsilon)} (\langle \psi_+ | d | \psi_+ \rangle + \langle \psi_- | d | \psi_- \rangle) \\ &= -2i \lim_{\epsilon \rightarrow 0} \int_{\gamma(\epsilon)} \langle \psi_+ | d | \psi_+ \rangle - 2\pi n \\ &= -2i \lim_{\epsilon \rightarrow 0} \int_{\gamma(\epsilon)} \langle \psi_- | d | \psi_- \rangle + 2\pi n, \end{aligned} \quad (5.37)$$

where n is the topological number given in (T), and $\gamma(\epsilon) \in S^2 - \{(0, 0, \pm 1)\}$ is the regularized curve in (3.26).

Hence, the geometric phase Δ_g of our model could be identified with the Berry phase for the two-level system. More precisely, the Gauss vector \mathbf{g} in $S^2 - \{(0, 0, \pm 1)\}$ corresponds to the eigenstates $|\psi_{\pm}\rangle$ in the *Bloch sphere*, and one-form $\cos \beta d\theta$ can be interpreted as the Berry connection $\langle \psi_{\pm} | d | \psi_{\pm} \rangle$. See Tab. 3.

6 Concluding remarks

In this article, we have focused on a simple kinematic toy model exhibiting the geometric phases. That is, a rotating disc around a fixed disc without slipping on the edge. The question is how much the moving disc has rotated. The total rotation angle consists of

Table 3: The correspondence between our model and the Berry phase

Our model	Berry phase
S^2	Bloch sphere
$\mathbf{g} \in S^2 - (0, 0, \pm 1)$	$ \psi_{\pm}\rangle \in \mathbb{C}^2$
$\frac{i}{2}(\pm 1 + \cos \beta)d\theta$	$\langle \psi_{\pm} d \psi_{\pm} \rangle$

the dynamical phase Δ_d and the geometric phase Δ_g . The latter is given by Thm. 3.15, and the answer to the question is given in (3.64). To verify these claims, the Baumkuchen lemma Lem. 3.1 has played a crucial role. Furthermore, with the use of the Gauss vector (3.21) and the regularized trajectory (3.26), we have obtained the main theorem Thm. 3.15. In § 4, we have demonstrated how our theory fits some concrete cases.

In § 5, we have discussed the important models sharing the common structure, which include Foucault's pendulum, Dirac's monopole potentials, and Berry phases. This fact implies that the underlying mathematical structure is the *Hopf fibration*,

$$S^1 \hookrightarrow S^3 \xrightarrow{\pi} S^2, \quad (6.1)$$

which is the principal fiber bundle equipped with $U(1)$ fiber embedded in the total space S^3 and the projection called the *Hopf map* $\pi : S^3 \rightarrow S^2$. In this picture, the geometric phase Δ_g will be given by the holonomy of Hopf fibration. We shall report this aspect in the near future.

Acknowledgment

We appreciate Osaka Central Advanced Mathematical Institute and Graduate School of Mathematics, Nagoya University as the hosts of the 32nd Japan Mathematics Contest and the 25th Japan Junior Mathematics Contest 2022, in which we have proposed our model as one of the problems [18]. We are grateful to our colleagues, Prof. Yoshiyuki Koga, Prof. Mitsutaka Kumakura, Prof. Yuki Sato, and Prof. Hiroshi Wakui for their communications with the subject of this article. TM also thanks Prof. Yuji Satoh for his careful reading of the manuscript and valuable comments. The work of TM was supported by JSPS KAKENHI Grant Number JP19K03421 and JP24K06665.

A Alternative proof of Theorem 3.15

Theorem 3.15 can also be proved by directly evaluating the right hand side of the line integral (3.28),

$$\Delta_g = \lim_{\epsilon \rightarrow 0} \int_{\gamma(\epsilon)} \cos \beta_\epsilon d\theta. \quad (\text{A.1})$$

Here, we only consider the case that γ is simple and surrounding the north pole $(0, 0, 1)$ on the left side, that is,

$$(I_+, I_-) = (1, 1). \quad (\text{A.2})$$

The proof for the other cases is almost parallel. In this case, for sufficiently small $\epsilon > 0$, we may assume that $\gamma(\epsilon) = \gamma$. Thus, it is enough to evaluate

$$\Delta_g = \int_{\gamma} \cos \beta d\theta. \quad (\text{A.3})$$

Because the local coordinate (θ, β) is degenerated at $\beta = 0, \pi$, we need to remove these poles to apply the Stokes' theorem. For this purpose, we consider the sufficiently small disc δ covering the north pole and decompose the integral contour as follows (see Fig. 17),

$$\int_{\gamma} \cos \beta d\theta = \int_{\gamma - \partial\delta} \cos \beta d\theta + \int_{\partial\delta} \cos \beta d\theta. \quad (\text{A.4})$$

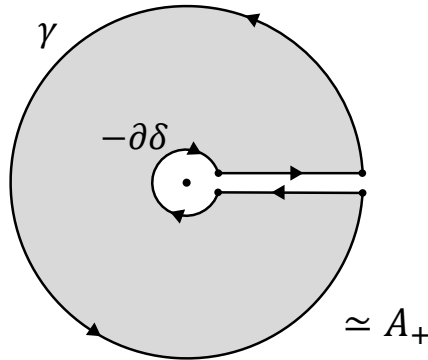


Figure 17: The contour $\gamma - \partial\delta$. The area in gray approaches to A_+ as δ shrinks to the north pole.

The first terms on the right hand side can be evaluated by the Stokes' theorem as

$$\int_{\gamma-\partial\delta} \cos \beta d\theta = \int_{S_+-\delta} d(\cos \beta d\theta) = \int_{S_+-\delta} \sin \beta d\theta \wedge d\beta. \quad (\text{A.5})$$

This gives the area of $S_+ - \delta$ and reduces A_+ as δ retracts to $(0, 0, 1)$. Hence, it holds that

$$\int_{\gamma-\partial\delta} \cos \beta d\theta \simeq A_+ \quad \text{as} \quad \delta \rightarrow (0, 0, 1). \quad (\text{A.6})$$

On the other hand, the second term is calculated as

$$\int_{\partial\delta} \cos \beta d\theta \simeq - \int_{\partial\delta} d\theta = -2\pi, \quad (\text{A.7})$$

because $\beta \simeq \pi$ when δ is sufficiently small region around $(0, 0, 1)$.

Since the decomposition (A.4) is independent of the size δ , it turns out to be

$$\int_{\gamma} \cos \beta d\theta = A_+ - 2\pi. \quad (\text{A.8})$$

This is the desired result for the present case,

$$\Delta_g = A_+ - 2\pi I_+ \quad \text{with} \quad I_+ = 1. \quad (\text{A.9})$$

B Baumkuchen angle and the geodesic curvature

It is worth clarifying the relation between Baumkuchen lemma 3.1 and the geodesic curvature in Def. 3.9. First, let us introduce a curve γ_q , which is locally parallel but separated by distance q from the curve γ , that is,

$$\gamma_q = \{ \mathbf{g}(s) - q\boldsymbol{\nu}(s) \in S^2 \mid s \in [0, L] \} \subset S^2, \quad (\text{B.1})$$

where L is the length of γ . Then, the length of the curve γ_q which we denote by L_q , is given by

$$L_q = \int_0^L |\mathbf{g}'(s) - q\boldsymbol{\nu}'(s)| ds. \quad (\text{B.2})$$

Note that $L_0 = L$ since $\gamma_0 = \gamma$.

Proposition B.1. *Suppose that the curve γ is smooth. Then, it holds that*

$$\lim_{q \rightarrow 0} \frac{L_q - L_0}{q} = \int_0^L \kappa_g(s) ds. \quad (\text{B.3})$$

Proof. Substituting (B.2) into the left hand side, it is calculated as

$$\begin{aligned}
\lim_{q \rightarrow 0} \frac{L_q - L_0}{q} \Big|_{q=0} &= \frac{d}{dq} L_q \Big|_{q=0} \\
&= \frac{d}{dq} \int_0^L |\mathbf{g}'(s) - q\boldsymbol{\nu}'(s)| ds \Big|_{q=0} \\
&= \int_0^L \frac{\partial}{\partial q} |\mathbf{g}'(s) - q\boldsymbol{\nu}'(s)| \Big|_{q=0} ds \\
&= \int_0^L \frac{-\mathbf{g}'(s) \cdot \boldsymbol{\nu}'(s) + q\boldsymbol{\nu}'(s) \cdot \boldsymbol{\nu}'(s)}{|\mathbf{g}'(s) + q\boldsymbol{\nu}'(s)|} \Big|_{q=0} ds \\
&= - \int_0^L \mathbf{g}'(s) \cdot \boldsymbol{\nu}'(s) ds .
\end{aligned} \tag{B.4}$$

where we have used $|\mathbf{g}'(s)| = 1$ in the last equality. Due to the relation (3.45) and the definition of κ_g in (3.46), we obtain the desired relation

$$\lim_{q \rightarrow 0} \frac{L_q - L_0}{q} \Big|_{q=0} = \int_0^L \mathbf{g}''(s) \cdot \boldsymbol{\nu}(s) ds = \int_0^L \kappa_g(s) ds . \tag{B.5}$$

This proves the proposition. \square

Remark B.2. The relation (B.3) could be regarded as the generalization of Baumkuhen lemma 3.1. To compare with Lem.3.1, suppose that the curve γ is a part of a circle, namely an arc, and the distance between two arcs q is smaller than the radius of the circle, r . Then, (B.3) becomes

$$\frac{L_q - L_0}{q} = \kappa_g L \tag{B.6}$$

as κ_g is constant. Notice that, by Baumkuchen lemma 3.1, the left hand side is equal to the angle θ_B of a piece of Baumkuchen, *i.e.*,

$$\frac{L_q - L_0}{q} = \frac{(r - q)\theta_B - r\theta_B}{q} = -\theta_B . \tag{B.7}$$

As $L = L_0 = r\theta_B$ on the right hand side, the equation (B.6) turns out to be

$$\kappa_g = -\frac{1}{r} . \tag{B.8}$$

This is indeed the curvature of a circle with radius r up to the sign. This discrepancy is just owing to our conventions for the Baumkuchen angle θ_B and the geodesic curvature κ_g . Hence, Prop.B.1 is the natural generalization of Baumkuchen lemma 3.1.

Remark B.3. The relation (B.3) holds not only for $\gamma \subset S^2$ but also for an arbitrary smooth curve in a two-dimensional smooth surface in \mathbb{R}^3 .

At the end of this section, let us apply Prop. B.1 to Thm. 3.11.

Corollary B.4. *Suppose that γ is a simple closed curve and smooth, and winding the north pole $(0, 0, 1)$ on the left side, i.e., $(I_+, I_-) = (1, 1)$. Then, the geometric phase is given by*

$$\Delta_g = \lim_{q \rightarrow 0} \frac{L_0 - L_q}{q}. \quad (\text{B.9})$$

Furthermore, when β is constant, it reduces to

$$\Delta_g = 2\pi \cos \beta. \quad (\text{B.10})$$

Proof. Plugging (B.3) with (3.52), we have

$$\Delta_g = \lim_{\epsilon \rightarrow 0} \int_{\gamma(\epsilon)} d\varphi - \lim_{q \rightarrow 0} \frac{L_q - L_0}{q} - \sum_{i=1}^n \alpha_i. \quad (\text{B.11})$$

When γ is a simple closed curve and smooth, and $(I_+, I_-) = (1, 1)$, the first and third terms vanish. Then, it becomes

$$\Delta_g = \lim_{q \rightarrow 0} \frac{L_0 - L_q}{q}. \quad (\text{B.12})$$

In addition, when β is constant, γ is a circle of radius $\sin \beta - q \cos \beta$. In this case, we get

$$L_q = 2\pi(\sin \beta - q \cos \beta). \quad (\text{B.13})$$

Substituting this into the above, we get

$$\Delta_g = \lim_{q \rightarrow 0} \frac{L_0 - L_q}{q} = 2\pi \cos \beta. \quad (\text{B.14})$$

□

It is noted that the expression (B.10) coincides with (4.76) of the example (iv) that we have discussed in §4. Since the example (iv) corresponds to Foucault's pendulum discussed in §5.1, Cor. B.4 also provides a simple proof of the Foucault's sine law (5.1) with the appropriate identifications in Tab. 2.

References

- [1] S. Pancharatnam, "Generalized theory of interference, and its applications," Proc. Indian Acad. Sci. A **44** (1956) no.5, 247-262.
- [2] H. C. Longuet-Higgins, U. Opik, M. H. L. Pryce, and R. A. Sack, "Studies of the Jahn-Teller Effect. II. The Dynamical Problem," Proceedings of the Royal Society of London Series A, 1958, feb, vol. 244, No. 1236, pp. 1-16,
- [3] J. H. Hannay, "Angle variable holonomy in adiabatic excursion of an integrable Hamiltonian," 1985 J. Phys. A: Math. Gen. 18 221.
- [4] M. V. Berry, "Quantal phase factors accompanying adiabatic changes," Proc. Roy. Soc. Lond. A **392** (1984), 45-57.
- [5] M. V. Berry, "The Quantum Phase, Five Years After," original contribution to [6] .
- [6] A. Shapere and F. Wilczek, "Geometric Phases in Physics," Advanced Series in Mathematical Physics Vol.5, World Scientific, Singapore, 1989.
- [7] S. Kobayashi and K. Nomizu, "Foundations of Differential Geometry Volume I,II" (1963, 1969), John Wiley & Sons.
- [8] N. Steenrod, "The Topology of Fibre Bundles" (1951), Princeton University Press.
- [9] M. Nakahara, "Geometry, Topology and Physics," Second edition (2003), CRC Press.
- [10] T. Eguchi, P. B. Gilkey and A. J. Hanson, "*Gravitation, Gauge Theories and Differential Geometry*," Phys. Rept. **66** (1980), 213.
- [11] H. Hopf, "Über die Abbildungen der dreidimensionalen Sphäre auf die Kugelfläche," Math. Ann. 104, 637–665 (1931).
- [12] P. A. M. Dirac, "Quantised singularities in the electromagnetic field," Proc. Roy. Soc. Lond. A **133** (1931) no.821, 60-72.
- [13] T. T. Wu and C. N. Yang, "Concept of Nonintegrable Phase Factors and Global Formulation of Gauge Fields," Phys. Rev. D **12** (1975), 3845-3857.
- [14] T. T. Wu and C. N. Yang, "Dirac Monopole Without Strings: Monopole Harmonics," Nucl. Phys. B **107** (1976), 365.
- [15] S. R. Coleman, "The magnetic monopole fifty years later," HUTP-82-A032, (97 pages, Part of Proceedings, Les Houches Summer School in Theoretical Physics: Gauge Theories in High Energy Physics - Session 37, Jun, 1982).

- [16] M. Minami, “Dirac’s Monopole and the Hopf Map,” *Progress of Theoretical Physics*, Vol. 62, No. 4, October 1979.
- [17] L. H. Ryder, “Dirac monopoles and the Hopf map S^3 to S^2 ,” *J. Phys. A* **13** (1980), 437-447.
- [18] T. Matsumoto, H. Takada, and O. Yasukura, The common problem “Rotation angles of the rotating disc,” the 32nd Japan Mathematics Contest and the 25th Japan Junior Mathematics Contest, 2022.
- [19] S. Ghosh, “Geometric Phases for Classical and Quantum Dynamics: Hannay Angle and Berry Phase for Loops on a Torus.” *Int J Theor Phys* 58, 2859–2871 (2019).
- [20] Jean Bernard Léon Foucault, “Démonstration physique du mouvement de rotation de la Terre au moyen du pendule,” *Comptes rendus hebdomadaires des séances de l’Académie des sciences*, Tome 32, 1851 (p.135-138).
- [21] L. E. Goodman, A. R. Robinson, ”Effect of Finite Rotations on Gyroscopic Sensing Devices.” *ASME. J. Appl. Mech.* June 1958; 25(2): 210–213.
- [22] K. Blankinship, ”A new kinematic theorem for rotational motion,” *PLANS 2004. Position Location and Navigation Symposium (IEEE Cat. No.04CH37556)*, Monterey, CA, USA, 2004, pp. 285-295.
- [23] H. K. Onnes, “Nieuwe Bewijzen voor de aswenteling der aarde.” (Ph.D. dissertation) Groningen: Wolters, 1879.
- [24] E. O. Schulz-DuBois, ”Foucault Pendulum Experiment by Kamerlingh Onnes and degenerate perturbation theory,” (1970), *Am. J. Phys.* 38 (2): 173.
- [25] J. E. Marsden, O. M. O’Reilly, F. J. Wicklin, B. W. Zombros, “Symmetry, Stability, Geometric Phases, and Mechanical Integrators (Part I, II)” (1991), *Nonlinear Science Today* 1 (1) 4–11 and (2) 13-21.
- [26] F. Monroy-Perez, Anzaldo-Meneses, “Study of the Foucault pendulum within the geometric control theory perspective,” *Cybernetics and Physics*, Vol. 1, No. 2, 2012, pp. 89-95.
- [27] J. E. Marsden, “Lectures on Mechanics,” *London Mathematical Society Lecture note series*, 174, Cambridge University Press (1992).
- [28] J. E. Marsden and T. Ratiu, “Introduction to Mechanics and Symmetry,” Springer-Verlag, New York. 17 (1999).

- [29] Jens von Bergmann, HsingChi von Bergmann, “Foucault pendulum through basic geometry,” *Am. J. Phys.* 1 October 2007; 75 (10): 888–892.
- [30] G. Reeb, “Les Solutions Périodiques De Certains Systèmes Différentiels Perturbés,” *Canadian Journal of Mathematics*. 1951;3:339-362.